Discovery of Small-Molecule Inhibitors of Receptor Activator of Nuclear Factor-κB Ligand (RANKL) with Superior Therapeutic Index

Vagelis Rinotas,[1,2] Athanasios Papakyriakou,[3] Foteini Violitzi,[2] Christos Papaneophytou,[4,5] Maria-Dimitra Ouzouni,[6] Polyxeni Alexiou,[6] Alexandros Strongilos,[7] Elias Couladouros,[6] George Kontopidis,[4] Elias Eliopoulos,[1] Eleni Douni[1,2,*]

[1]Laboratory of Genetics, Department of Biotechnology, Agricultural University of Athens, 75 Iera Odos, 11855, Athens, Greece

[2]Institute for Bioinnovation, Biomedical Sciences Research Center "Alexander Fleming", 34 Fleming Street, 16672, Vari, Greece

[3]Institute of Biosciences and Applications, National Centre for Scientific Research "Demokritos", 15341, Agia Paraskevi, Athens, Greece

[4]Department of Biochemistry, Veterinary School, University of Thessaly, 224 Trikalon, 43131, Karditsa, Greece

[5]Department of Life and Health Sciences, School of Sciences and Engineering, University of Nicosia, 46 Makedonitissas Avenue, 2417, Nicosia, Cyprus

[6]Laboratory of General Chemistry, Department of Food Science and Human Nutrition, Agricultural University of Athens, 75 Iera Odos, 11855, Athens, Greece

[7]proACTINA SA, 20 Delfon Street, 15125, Marousi-Athens, Greece

Supporting Information

Table of Contents

Computational Results……S2-S8, S11-S17, S19-S23

Supplementary Biological Results……S9-S10, S18

Spectroscopic and LC/MS data for the new compounds…… S24-S41

Table S1. Re-docking results of SPD-304 against the TNF dimer using the X-ray coordinates from PDB ID: 2AZ5**.** For each cluster of bound conformations within a root-mean-square deviation (RMSD) of 2.0 Å, the number of poses (population), the lowest estimated binding energy (ΔG^{est}), and the lowest RMSD from the reference, crystallographic pose ($RMSD_{ref}$) are given. The clusters with the lowest $RMSD_{ref}$ (<2.0 Å) are highlighted.

Cluster Rank #	Cluster population		ΔG^{est} (Kcal/mol)	$RMSD_{ref}$ (Å)
1	2	##	-9.15	3.65
2	1	#	-8.66	3.70
3	1	#	-8.62	5.59
4	2	##	-8.59	4.29
5	10	##########	-8.56	3.79
6	5	#####	-8.31	3.48
7	2	##	-8.24	3.33
8	1	#	-8.22	3.19
9	2	##	-8.21	5.09
10	13	##############	-8.11	2.84
11	1	#	-8.11	4.76
12	2	##	-8.03	3.72
13	9	#########	-7.99	3.51
14	3	###	-7.98	3.44
15	1	#	-7.93	3.55
16	1	#	-7.81	4.04
17	1	#	-7.72	4.44
18	7	#######	-7.66	3.92
19	2	##	-7.63	3.93
20	**2**	**##**	**-7.60**	**1.03**
21	1	#	-7.40	3.94
22	2	##	-7.31	3.54
23	3	###	-7.30	2.03
24	1	#	-7.18	4.90
25	1	#	-7.08	4.30
26	1	#	-7.07	3.10
27	1	#	-7.06	2.69
28	2	##	-7.06	4.06
29	6	######	-6.99	2.52
30	1	#	-6.99	4.28
31	1	#	-6.94	3.70
32	1	#	-6.90	3.60
33	1	#	-6.88	3.02
34	1	#	-6.76	2.63
35	1	#	-6.68	2.47
36	1	#	-6.64	3.46
37	**1**	**#**	**-6.62**	**1.86**
38	1	#	-6.62	2.63
39	1	#	-6.55	2.49
40	1	#	-6.55	3.36
41	1	#	-6.40	3.09
42	2	##	-6.33	3.72

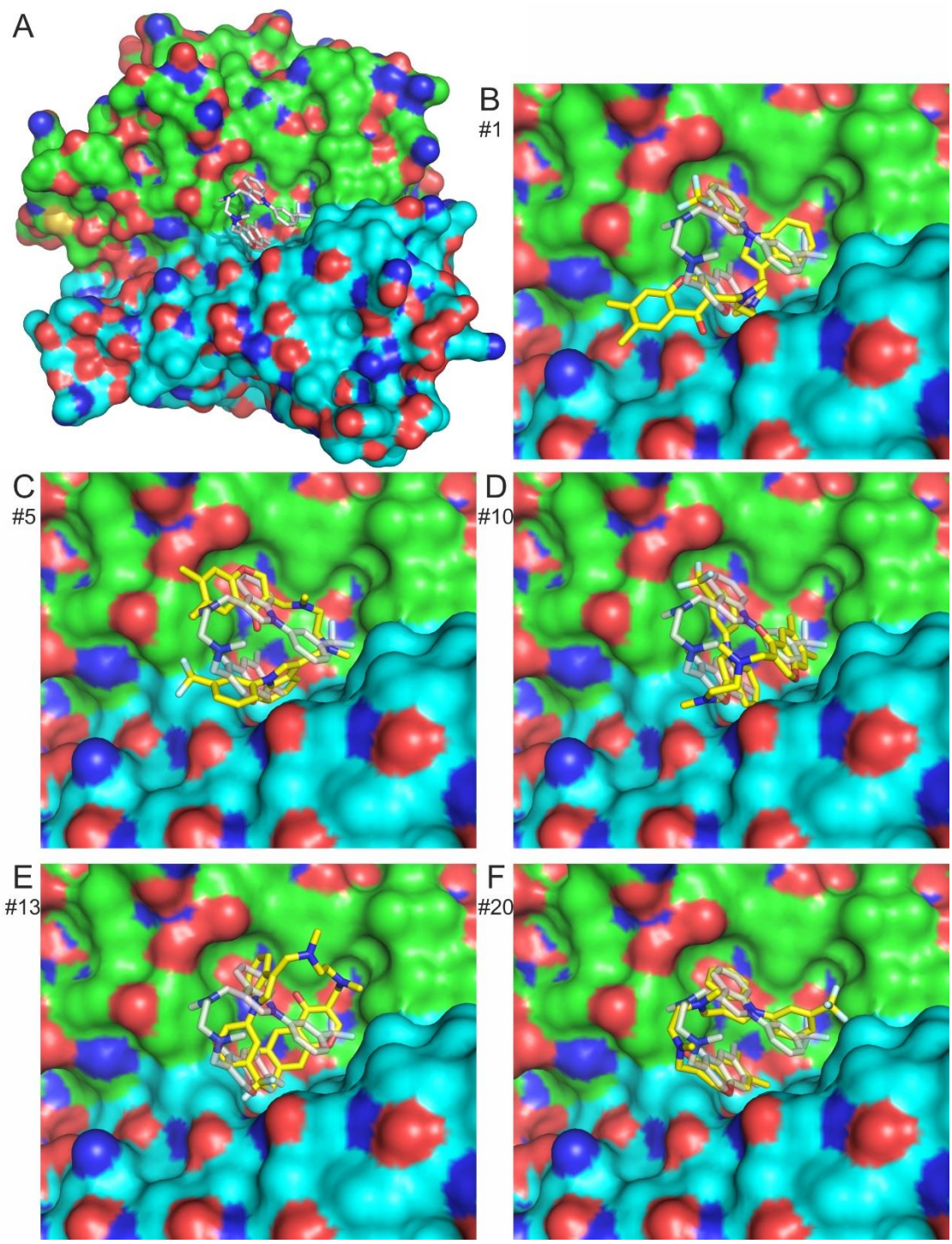

Figure S1. (A) Surface representation of the TNF dimer in complex with **SPD-304** (white-colored carbons) based on the X-ray structure (PDB ID: 2AZ5). (**B**) Close-up view of the interface pocket showing the top-ranked (#1) docked pose of **SPD-304** (yellow-colored carbons) in comparison with the X-ray pose. (**C–F**) 3 of the top-populated clusters of conformations ranked as cluster #5, #10 and #13 (**C, D, E**, respectively), and the lowest $RMSD_{ref}$ pose ranked at cluster #20 (**F**).

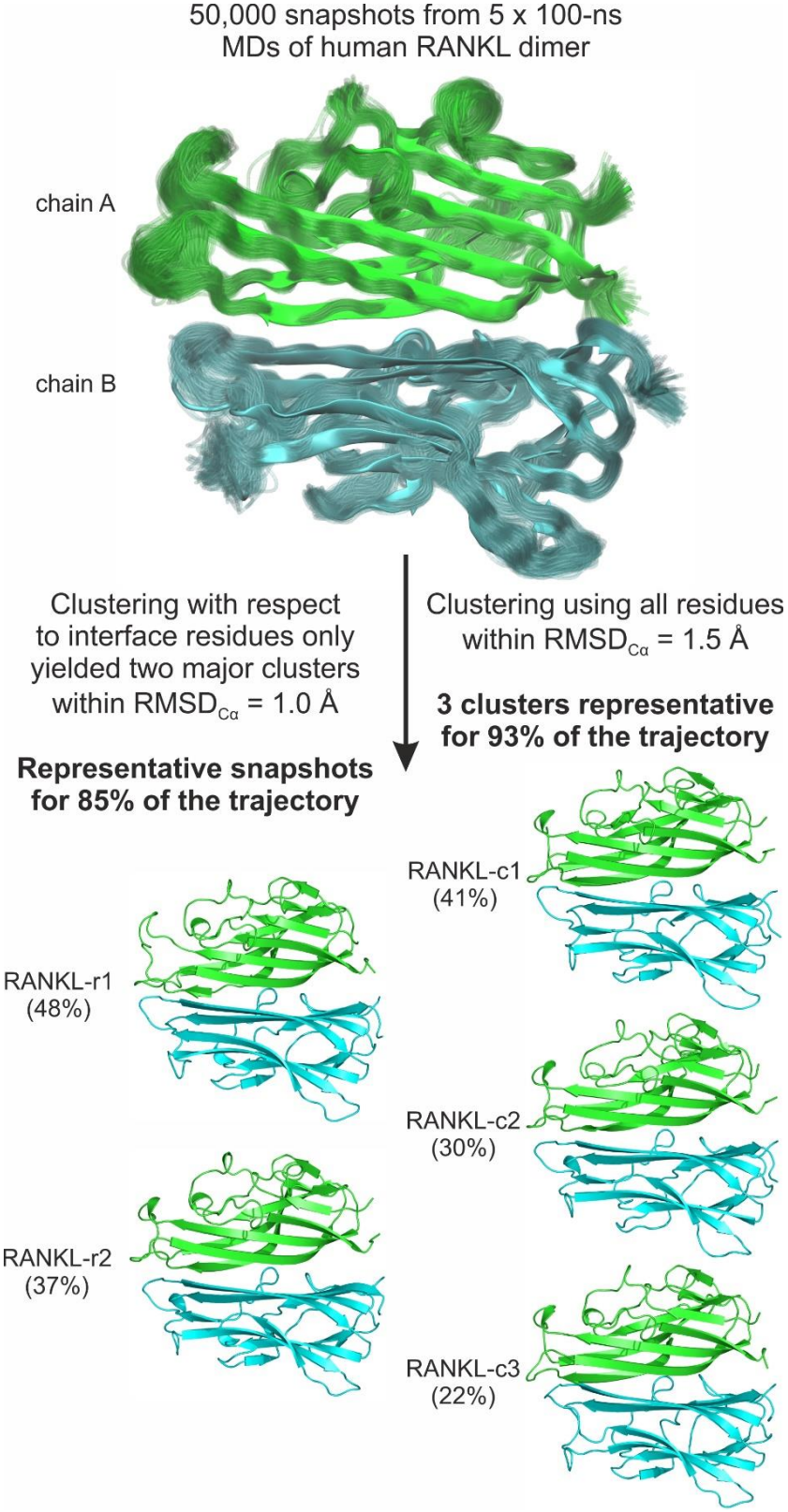

Figure S2.

Methodology for the extraction of representative snapshots from the MDs of human RANKL dimer, indicating the percent of the trajectory represented within each major cluster in parentheses.

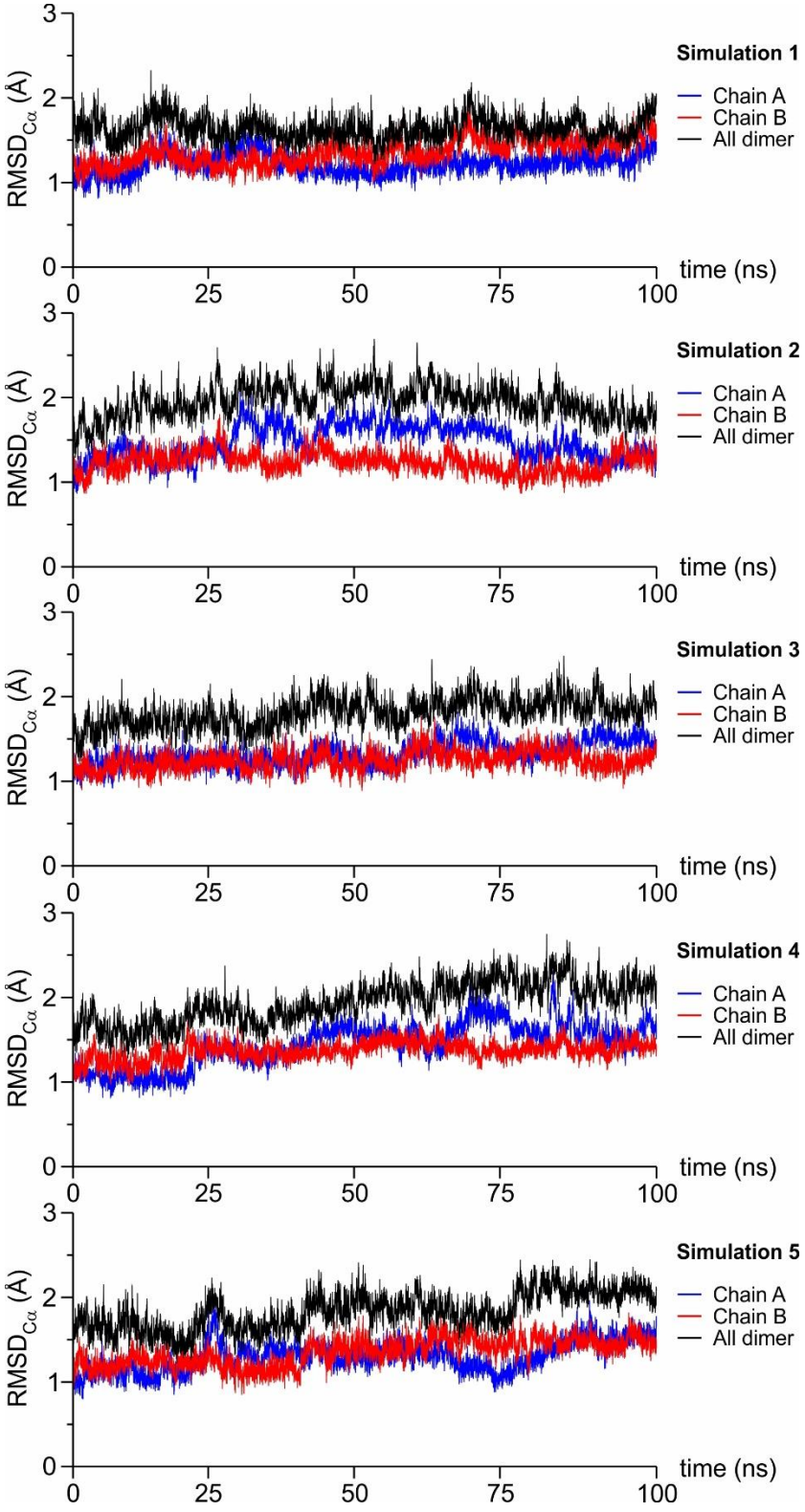

Figure S3. Plots of the root-mean-square deviation (RMSD) of the C_α atoms from the initial model of human RANKL dimer as a function of the MD time for the 5 simulations.

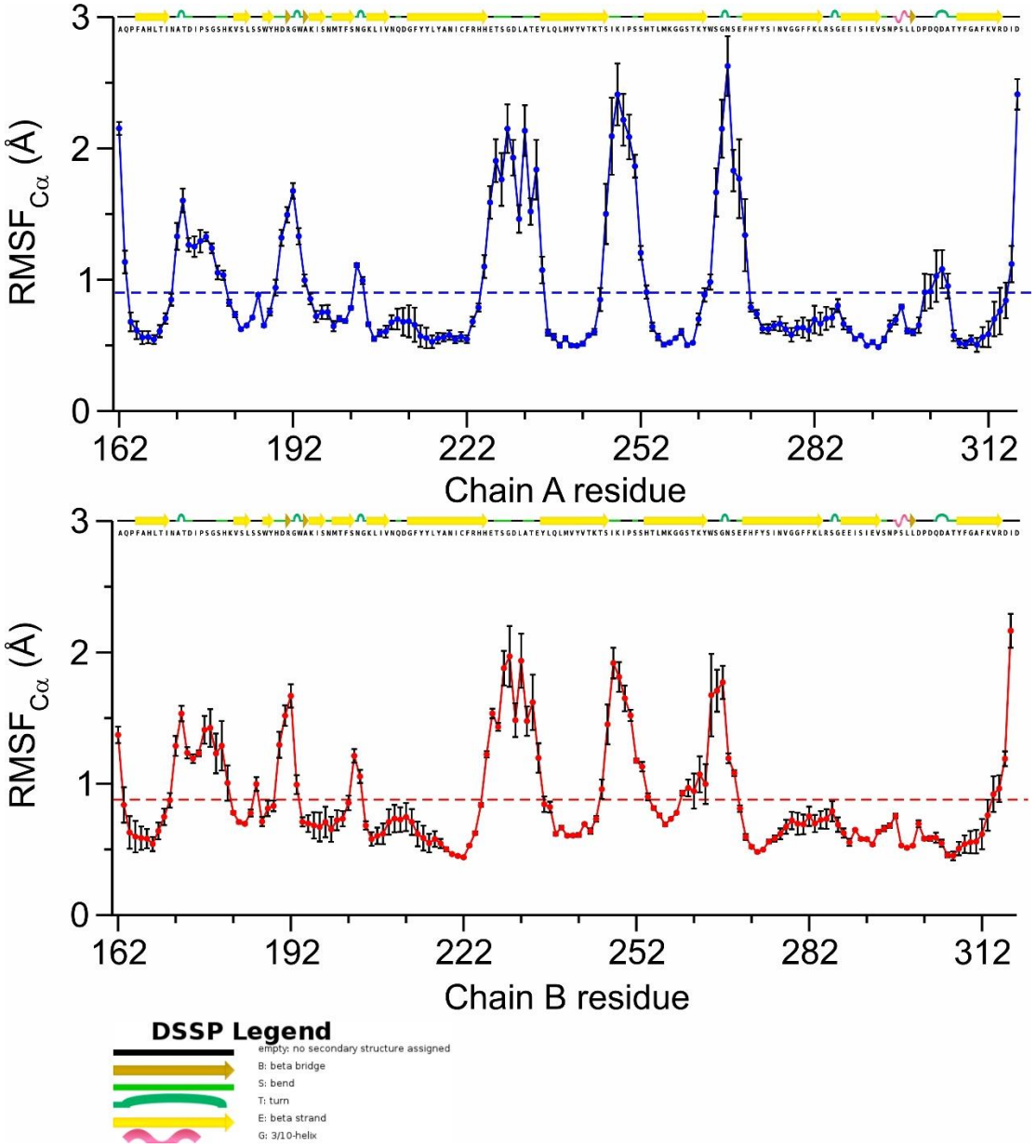

Figure S4. Plots of the mean atomic root-mean-square fluctuations (RMSF) of the C_α atoms for each chain of the human RANKL dimer model extracted from the 5 MD simulations. Error bars indicate the standard error of the mean (± SEM) and dashed lines indicate the average RMSF value for all residues. Inset, the DSSP assignment of the secondary structure as determined from the X-ray coordinates of the human RANKL/OPG complex (PDB ID: 3URF).

Table S2. Docking results of the 10 top-ranked clusters of conformations obtained for **SPD-304** against the 6 representative conformations of the human RANKL dimer model. The lowest and the mean binding energy, along with the number of conformations for each cluster are given.

Cluster Rank	Low. ΔG^{est} (Kcal/mol)	No. Conf.	Mean ΔG^{est} (Kcal/mol)
RANKL-min			
1	**-7.76**	**8**	**-7.04**
2	-7.72	5	-7.16
3	-7.19	2	-6.88
4	-7.12	1	-7.12
5	-6.89	4	-6.12
6	-6.89	1	-6.89
7	-6.86	2	-6.75
8	-6.74	6	-5.83
9	-6.71	6	-6.07
10	-6.66	2	-6.33
RANKL-r1			
1	-8.06	1	-8.06
2	**-8.04**	**3**	**-7.60**
3	-7.83	1	-7.83
4	-7.65	2	-7.51
5	-7.46	2	-7.29
6	-7.39	1	-7.39
7	-7.37	3	-6.89
8	-7.21	1	-7.21
9	-7.09	2	-6.80
10	-7.04	1	-7.04
RANKL-r2			
1	-8.57	3	-7.89
2	-8.02	1	-8.02
3	-8.00	4	-7.54
4	**-7.91**	**14**	**-6.46**
5	-7.86	2	-7.48
6	-7.69	2	-7.61
7	-7.58	4	-7.15
8	-7.57	2	-7.27
9	-7.56	2	-6.61
10	-7.40	1	-7.40

Cluster Rank	Low. ΔG^{est} (Kcal/mol)	No. Conf.	Mean ΔG^{est} (Kcal/mol)
RANKL-c1			
1	-9.28	2	-8.74
2	-8.62	2	-7.88
3	-8.13	1	-8.13
4	-7.97	3	-7.84
5	-7.90	2	-7.58
6	-7.73	1	-7.73
7	-7.54	1	-7.54
8	-7.45	2	-7.38
9	**-7.39**	**9**	**-6.34**
10	-7.38	1	-7.38
RANKL-c2			
1	**-8.80**	**6**	**-8.13**
2	-8.03	6	-6.86
3	-7.98	4	-7.11
4	-7.92	1	-7.92
5	-7.86	4	-7.42
6	-7.42	1	-7.42
7	-7.35	1	-7.35
8	-7.32	1	-7.32
9	-7.30	1	-7.30
10	-7.17	2	-6.59
RANKL-c3			
1	-8.08	1	-8.08
2	-7.94	4	-7.75
3	-7.88	4	-7.37
4	-7.71	2	-7.44
5	-7.57	1	-7.57
6	**-7.51**	**5**	**-7.08**
7	-7.38	1	-7.38
8	-7.33	1	-7.33
9	-7.31	2	-7.07
10	-7.12	2	-6.81

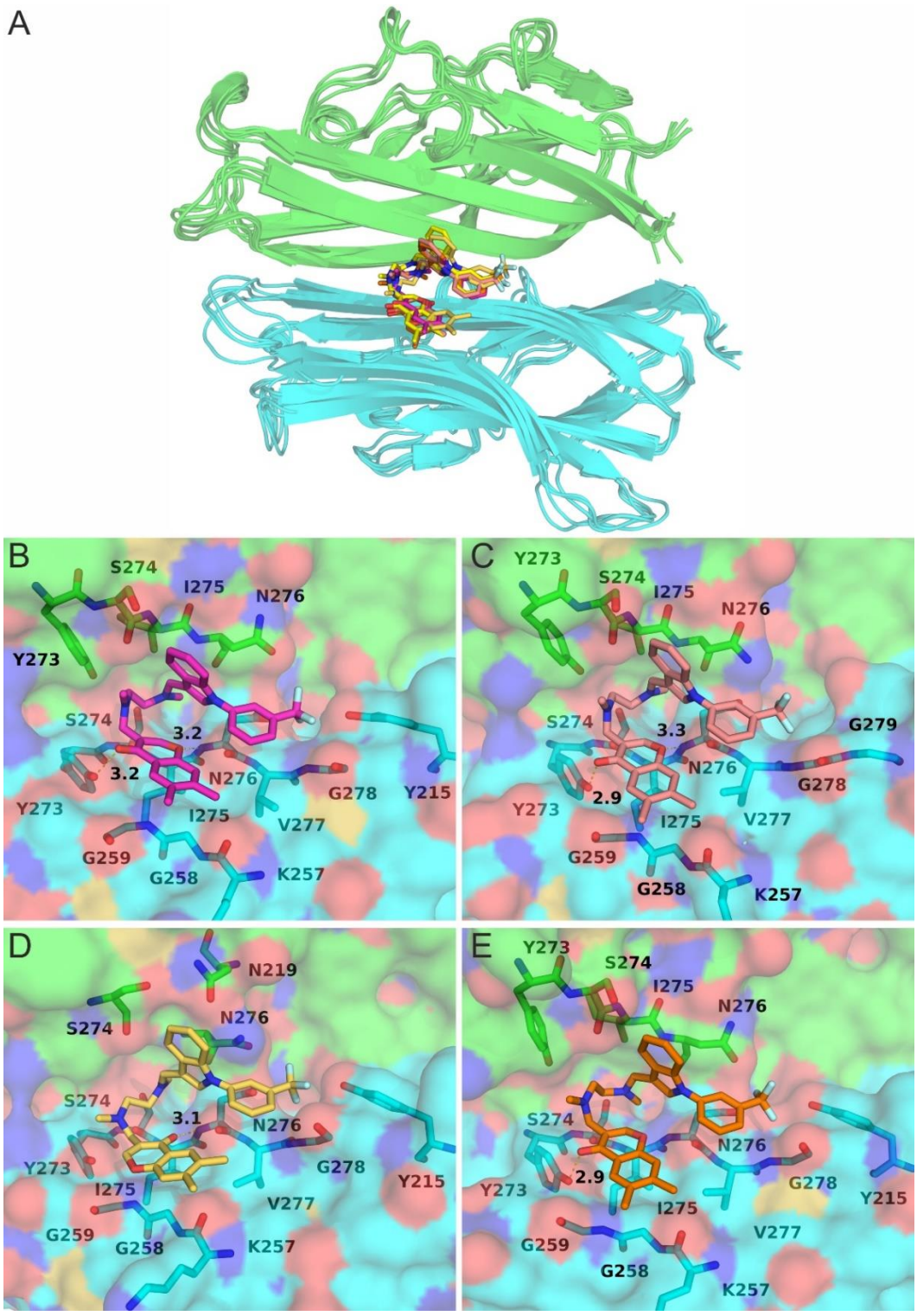

Figure S5. (A) Superposition of 5 similar, top-ranked bound poses of **SPD-304** in complex with representative models of human RANKL dimer. Close-up views of the binding interface from the corresponding models of RANKL-r2 (**B**), RANKL-c1 (**C**), RANKL-c2 (**D**), and RANKL-c3 (**E**).

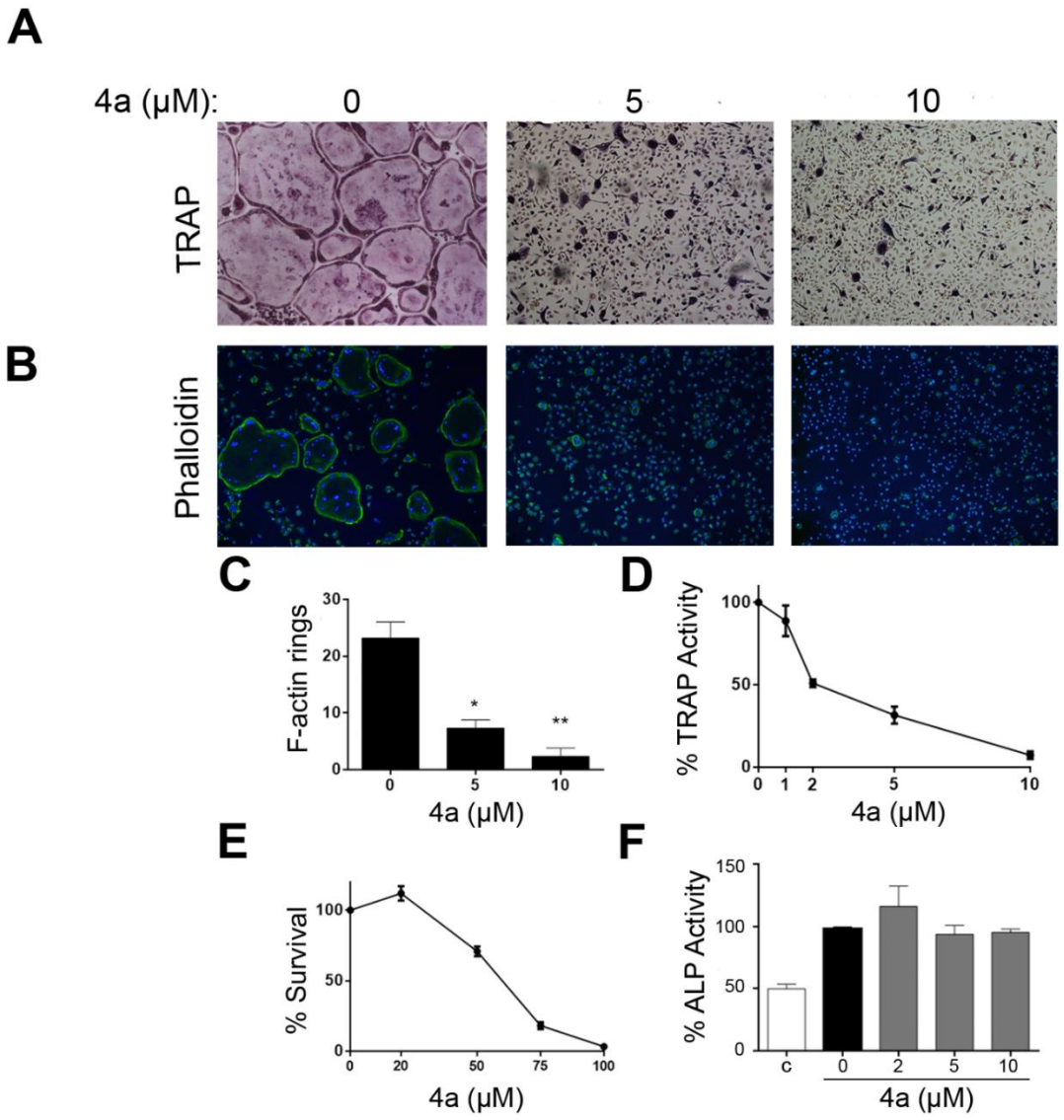

Figure S6. (**A**) Osteoclastogenesis cultures based on BM cells treated with compound **4a** at 5 and 10 μM in the presence of RANKL (40 ng/mL) and M-CSF (25 ng/mL) for 5 days upon staining with TRAP. (**B**) Actin ring organization in osteoclastogenesis cultures upon exposure compound **4a** at 5 and 10 μM as shown by phalloidin staining and DAPI. (**C**) Quantification of intact F-actin rings per mm2 on osteoclastogenesis cultures treated with compound **4a** at 5 and 10 μM. (**D**) IC_{50} calculation for compound **4a** effect on RANKL-induced osteoclastogenesis based on TRAP activity measured at day 4. (**E**) LC_{50} calculation of compound **4a** effect (0–100 μM) on BMM cell viability by MTT assay. (**F**) Effect of compound **4a** (2, 5 and 10 μM) on the differentiation of pre-osteoblastic MC3T3-E1 cells as measured by ALP activity. Results are presented as means ± SD (n>3). *p>0.05, **p>0.01.

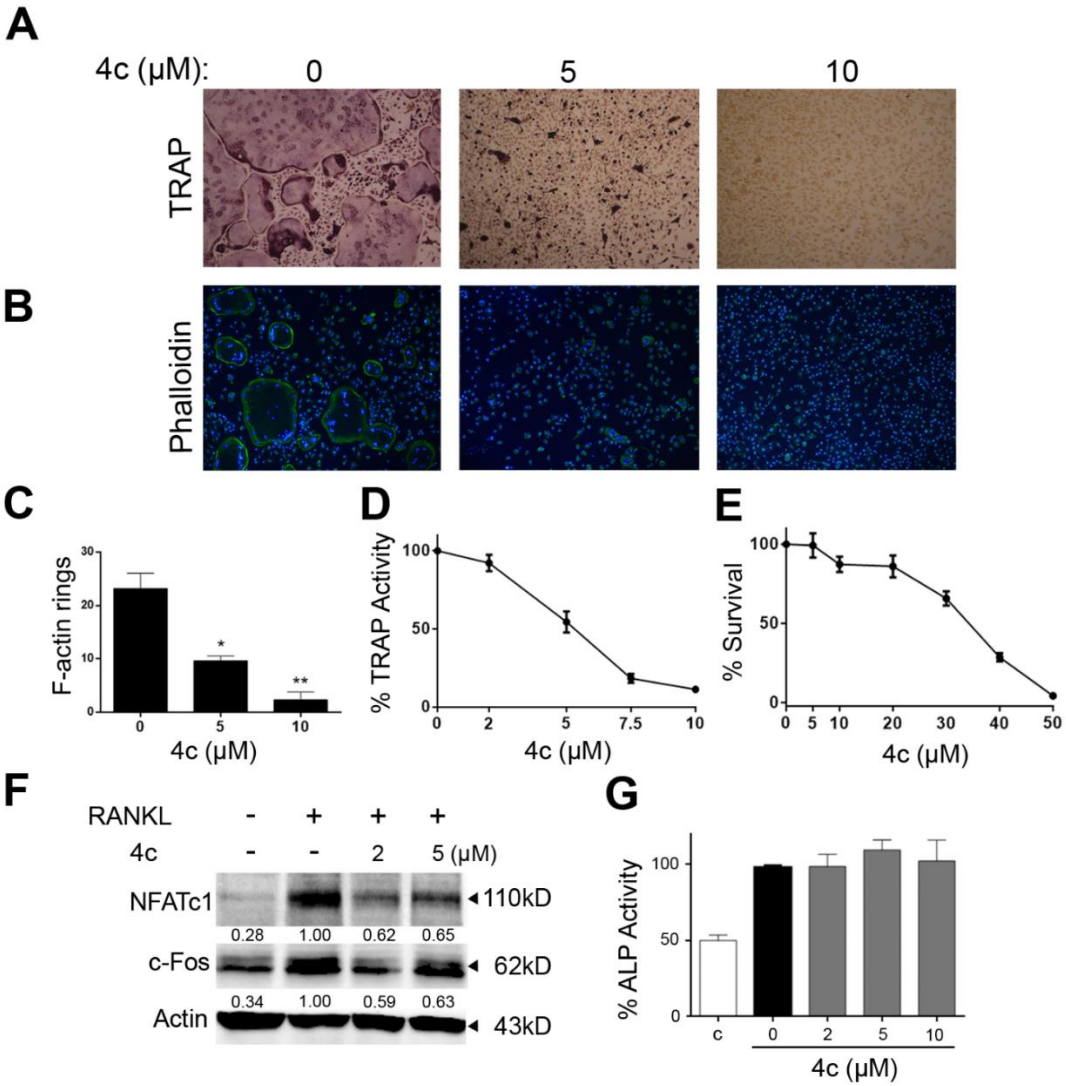

Figure S7. (**A**) Osteoclastogenesis assays treated with compound **4c** at 5 and 10 μM in the presence of RANKL (40 ng/mL) and M-CSF (25 ng/mL) for 5 days upon staining with TRAP. (**B**) Actin ring organization in osteoclastogenesis cultures upon exposure to compound **4c** at 5 and 10 μM as shown by phalloidin staining and DAPI. (**C**) Quantification of intact F-actin rings per mm^2 on osteoclastogenesis cultures treated with compound **4c** at 5 and 10 μM. (**D**) IC_{50} calculation for compound **4c** effect on RANKL-induced osteoclastogenesis based on TRAP activity measured at day 4. (**E**) LC_{50} calculation of compound **4c** effect (0–100 μM) on BMM cell viability by MTT assay. (**F**) Western blot showing the effect of preincubated compound **4c** with RANKL at the indicated concentrations on the induction of NFATc1 and c-Fos in RAW264.7 cells. (**G**) Effect of compound **4c** (2, 5 and 10 μM) on the differentiation of preosteoblastic MC3T3-E1 cells as measured by ALP activity. Results are presented as means ± SD (n>3). *p>0.05, **p>0.01.

Table S3. Docking results of the 10 top-ranked clusters of conformations obtained for compound **1b** against the 6 representative conformations of the human RANKL dimer model. The lowest and the mean binding energy, along with the number of conformations for each cluster are given.

Cluster Rank	Low. ΔG^{est} (Kcal/mol)	No. Conf.	Mean ΔG^{est} (Kcal/mol)
RANKL-min			
1	-8.41	2	-8.22
2	-8.27	6	-7.80
3	-8.27	2	-7.18
4	-8.21	7	-7.36
5	-8.09	2	-7.51
6	-7.88	5	-7.46
7	**-7.59**	**12**	**-6.91**
8	-7.46	1	-7.46
9	-7.37	4	-7.29
10	-7.34	1	-7.34
RANKL-r1			
1	**-8.72**	**12**	**-8.17**
2	-8.33	5	-7.73
3	-8.16	2	-7.73
4	-8.15	2	-7.98
5	-8.15	1	-8.15
6	-8.09	5	-7.55
7	-7.89	4	-7.39
8	-7.86	1	-7.86
9	-7.85	3	-7.54
10	-7.84	1	-7.84
RANKL-r2			
1	-8.85	6	-8.13
2	**-8.72**	**8**	**-7.82**
3	-8.43	7	-7.39
4	-8.40	8	-7.79
5	-8.37	1	-8.37
6	-8.24	3	-7.46
7	-7.94	1	-7.94
8	-7.84	1	-7.84
9	-7.82	1	-7.82
10	-7.77	2	-7.65

Cluster Rank	Low. ΔG^{est} (Kcal/mol)	No. Conf.	Mean ΔG^{est} (Kcal/mol)
RANKL-c1			
1	-8.53	1	-8.53
2	-8.46	6	-8.08
3	-8.38	1	-8.38
4	**-8.32**	**12**	**-7.84**
5	-8.04	1	-8.04
6	-7.94	7	-7.74
7	-7.78	4	-7.25
8	-7.74	3	-7.38
9	-7.70	2	-7.33
10	-7.62	1	-7.62
RANKL-c2			
1	-9.04	3	-8.36
2	-8.99	2	-8.34
3	-8.92	1	-8.92
4	**-8.85**	**4**	**-8.28**
5	-8.70	3	-8.39
6	-8.61	5	-7.97
7	-8.53	2	-8.14
8	-8.49	1	-8.49
9	-8.23	2	-7.90
10	-8.13	1	-8.13
RANKL-c3			
1	**-9.60**	**11**	**-8.63**
2	-9.09	3	-8.26
3	-8.72	8	-8.30
4	-8.60	4	-7.78
5	-8.48	1	-8.48
6	-8.33	1	-8.33
7	-8.28	2	-7.63
8	-8.22	2	-8.18
9	-7.85	1	-7.85
10	-7.78	1	-7.78

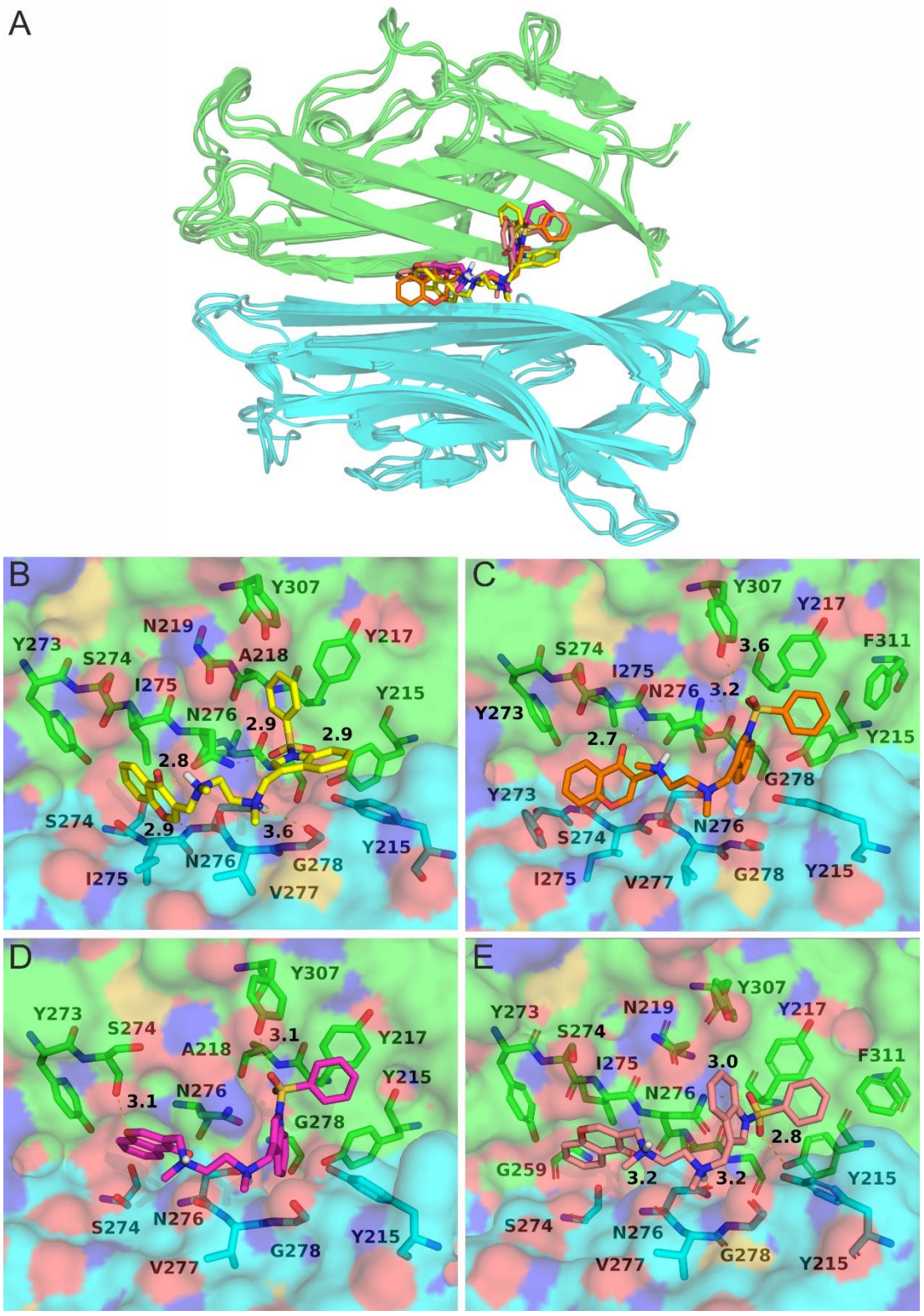

Figure S8. (A) Superposition of 4 similar, top-ranked bound poses of **1b** in complex with representative models of human RANKL dimer. Close-up views of the binding interface from the model of RANKL-r1 (**B**), RANKL-r2 (**C**), RANKL-c2 (**D**) and RANKL-c3 (**E**) with the corresponding bound pose of compound **1b**.

Table S4. Docking results of the 10 top-ranked clusters of conformations obtained for compound **4a** against the 6 representative conformations of the human RANKL dimer model. The lowest and the mean binding energy, along with the number of conformations for each cluster are given.

Cluster Rank	Low. ΔG^{est} (Kcal/mol)	No. Conf.	Mean ΔG^{est} (Kcal/mol)
RANKL-min			
1	-8.32	6	-7.79
2	-8.30	6	-8.09
3	**-8.27**	**8**	**-7.69**
4	-8.26	2	-8.18
5	-8.16	3	-7.45
6	-8.13	1	-8.13
7	-8.11	1	-8.11
8	-8.03	1	-8.03
9	-7.91	1	-7.91
10	-7.91	2	-7.49
RANKL-r1			
1	**-10.30**	**20**	**-8.91**
2	-9.75	3	-9.49
3	-9.27	2	-8.70
4	-8.83	9	-7.92
5	-8.64	1	-8.64
6	-8.56	2	-8.19
7	-8.53	1	-8.53
8	-8.52	8	-7.85
9	-8.35	4	-7.96
10	-8.20	2	-8.18
RANKL-r2			
1	**-8.98**	**8**	**-8.65**
2	-8.79	6	-8.45
3	-8.64	5	-8.41
4	-8.45	1	-8.45
5	-8.37	4	-8.18
6	-8.34	2	-8.32
7	-8.31	1	-8.31
8	-8.29	2	-8.02
9	-8.29	1	-8.29
10	-8.24	4	-7.83

Cluster Rank	Low. ΔG^{est} (Kcal/mol)	No. Conf.	Mean ΔG^{est} (Kcal/mol)
RANKL-c1			
1	-9.93	6	-9.18
2	-9.22	1	-9.22
3	-8.72	1	-8.72
4	-8.65	3	-8.01
5	-8.63	1	-8.63
6	**-8.62**	**14**	**-8.00**
7	-8.34	7	-8.15
8	-8.34	3	-8.14
9	-8.26	3	-7.99
10	-8.13	2	-7.68
RANKL-c2			
1	-9.85	6	-9.33
2	**-9.16**	**23**	**-8.48**
3	-8.88	6	-8.45
4	-8.71	9	-8.45
5	-8.70	3	-8.36
6	-8.45	2	-7.97
7	-8.43	5	-8.20
8	-8.40	2	-8.17
9	-8.36	2	-8.20
10	-8.34	2	-7.96
RANKL-c3			
1	**-9.68**	**15**	**-8.84**
2	-9.38	10	-8.38
3	-8.89	3	-8.65
4	-8.89	3	-8.77
5	-8.88	5	-8.37
6	-8.86	10	-8.15
7	-8.85	1	-8.85
8	-8.59	2	-8.37
9	-8.54	2	-8.51
10	-8.20	2	-8.20

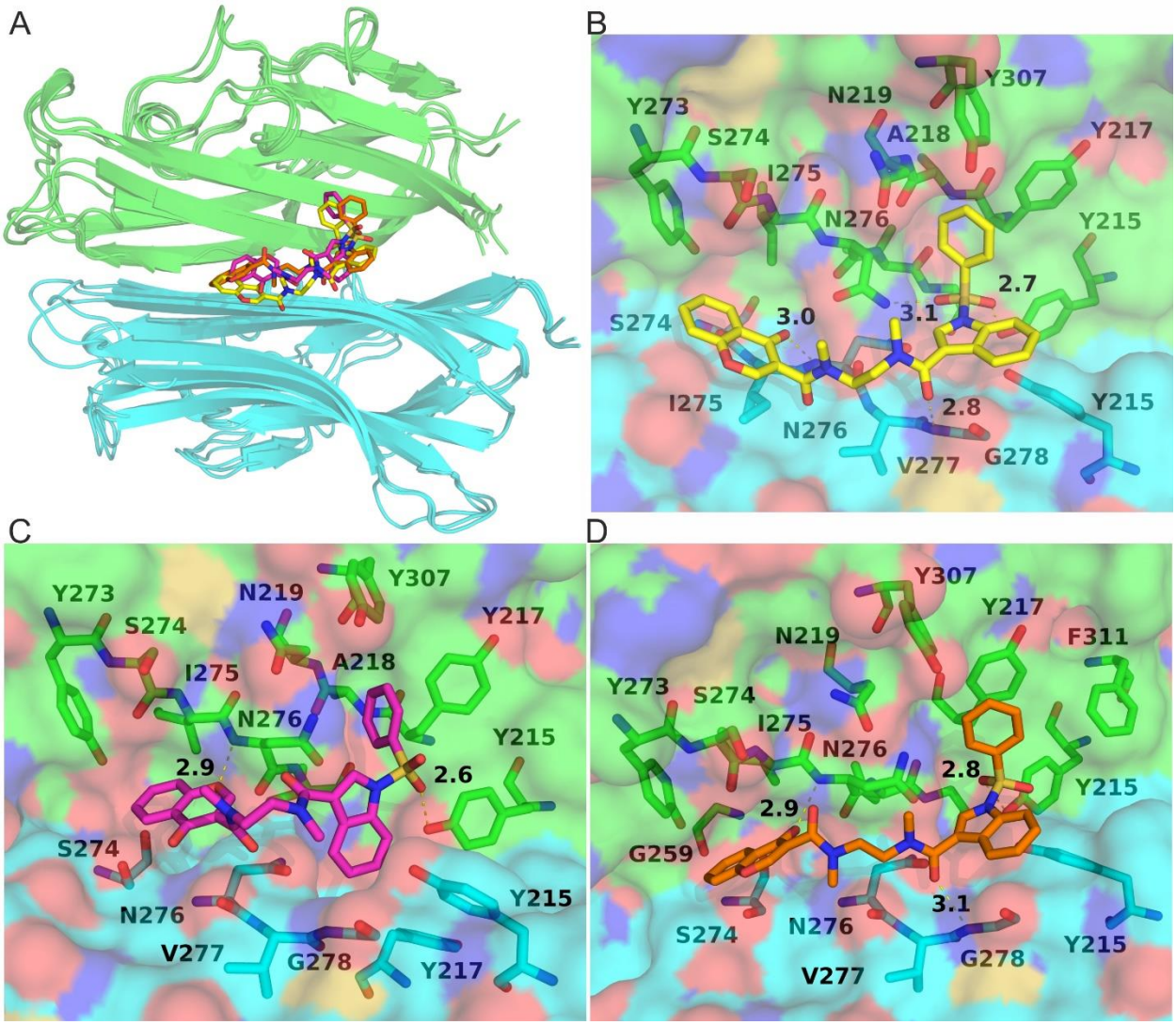

Figure S9. (A) Superposition of 3 similar, top-ranked bound poses of **4a** in complex with representative models of human RANKL dimer. Close-up views of the binding interface from the model of RANKL-r1 (**B**), RANKL-min (**C**), and RANKL-c3 (**D**) with the corresponding bound pose of **4a**.

Table S5. Docking results of the 10 top-ranked clusters of conformations obtained for compound **3b** against the 6 representative conformations of the human RANKL dimer model. The lowest and the mean binding energy, along with the number of conformations for each cluster are given.

Cluster Rank	Low. ΔG^{est} (Kcal/mol)	No. Conf.	Mean ΔG^{est} (Kcal/mol)
RANKL-min			
1	-9.61	6	-8.59
2	**-9.25**	**13**	**-8.85**
3	-8.74	7	-8.47
4	-8.65	5	-8.05
5	-8.42	1	-8.42
6	-8.42	7	-8.01
7	-8.38	1	-8.38
8	-8.32	6	-8.02
9	-8.24	5	-8.17
10	-8.24	2	-7.77
RANKL-r1			
1	-10.26	8	-9.62
2	**-10.21**	**16**	**-9.19**
3	-10.12	5	-9.67
4	-9.74	4	-9.16
5	-9.61	2	-9.43
6	-9.53	5	-8.71
7	-9.43	3	-9.20
8	-9.26	8	-8.71
9	-9.24	3	-9.17
10	-9.22	2	-9.02
RANKL-r2			
1	**-11.00**	**50**	**-10.44**
2	-10.53	17	-9.97
3	-9.94	8	-9.28
4	-9.81	1	-9.81
5	-9.66	11	-9.43
6	-9.50	1	-9.50
7	-9.41	2	-9.27
8	-8.93	1	-8.93
9	-8.86	1	-8.86
10	-8.82	4	-8.47

Cluster Rank	Low. ΔG^{est} (Kcal/mol)	No. Conf.	Mean ΔG^{est} (Kcal/mol)
RANKL-c1			
1	**-10.95**	**26**	**-10.21**
2	-10.72	12	-9.96
3	-10.62	6	-9.90
4	-10.58	7	-9.88
5	-10.35	2	-9.34
6	-10.15	5	-10.05
7	-10.12	9	-9.64
8	-9.83	4	-9.58
9	-9.78	4	-9.63
10	-9.78	5	-9.48
RANKL-c2			
1	**-11.30**	**52**	**-10.68**
2	-11.25	6	-10.54
3	-10.55	7	-10.16
4	-9.54	1	-9.54
5	-9.52	2	-9.48
6	-9.48	2	-9.47
7	-9.41	3	-9.20
8	-9.41	4	-9.33
9	-9.26	4	-9.11
10	-9.20	1	-9.20
RANKL-c3			
1	-9.64	6	-8.95
2	-9.15	6	-8.43
3	**-9.09**	**16**	**-8.27**
4	-9.05	4	-8.62
5	-8.82	4	-8.63
6	-8.81	2	-8.51
7	-8.75	2	-8.57
8	-8.75	3	-8.46
9	-8.69	1	-8.69
10	-8.67	1	-8.67

Table S6. Docking results of the 10 top-ranked clusters of conformations obtained for compound **4c** against the 6 representative conformations of the human RANKL dimer model. The lowest and the mean binding energy, along with the number of conformations for each cluster are given.

Cluster Rank	Low. ΔG^{est} (Kcal/mol)	No. Conf.	Mean ΔG^{est} (Kcal/mol)
RANKL-min			
1	-9.70	8	-9.10
2	-9.65	9	-8.76
3	**-8.91**	**12**	**-8.38**
4	-8.87	1	-8.87
5	-8.86	4	-8.51
6	-8.75	3	-8.59
7	-8.73	4	-8.39
8	-8.51	1	-8.51
9	-8.40	1	-8.40
10	-8.35	2	-7.95
RANKL-r1			
1	-9.99	1	-9.99
2	-9.88	5	-9.30
3	-9.77	9	-8.78
4	**-9.69**	**9**	**-9.34**
5	-9.65	1	-9.65
6	-9.62	2	-9.56
7	-9.61	1	-9.61
8	-9.45	2	-9.39
9	-9.42	2	-8.95
10	-9.25	2	-9.04
RANKL-r2			
1	**-10.58**	**17**	**-9.79**
2	-10.12	7	-9.51
3	-9.87	7	-9.54
4	-9.78	1	-9.78
5	-9.77	4	-9.46
6	-9.76	5	-8.92
7	-9.62	4	-8.97
8	-9.40	2	-9.11
9	-9.28	1	-9.28
10	-9.21	3	-8.75

Cluster Rank	Low. ΔG^{est} (Kcal/mol)	No. Conf.	Mean ΔG^{est} (Kcal/mol)
RANKL-c1			
1	-10.77	10	-9.94
2	-10.69	3	-9.99
3	**-10.51**	**19**	**-9.96**
4	-10.35	5	-9.61
5	-10.16	2	-10.12
6	-10.08	3	-9.72
7	-9.96	4	-9.45
8	-9.51	2	-9.22
9	-9.45	1	-9.45
10	-9.44	1	-9.44
RANKL-c2			
1	-10.87	9	-9.47
2	-10.79	5	-9.60
3	**-10.29**	**11**	**-9.30**
4	-10.13	4	-9.36
5	-10.09	8	-9.44
6	-10.00	8	-9.50
7	-9.92	4	-9.60
8	-9.83	6	-9.47
9	-9.75	1	-9.75
10	-9.65	1	-9.65
RANKL-c3			
1	**-9.78**	**12**	**-9.14**
2	-9.68	10	-9.03
3	-9.61	4	-9.12
4	-9.48	1	-9.48
5	-9.39	5	-8.71
6	-9.18	7	-8.58
7	-9.02	4	-8.81
8	-8.95	1	-8.95
9	-8.90	1	-8.90
10	-8.86	4	-7.54

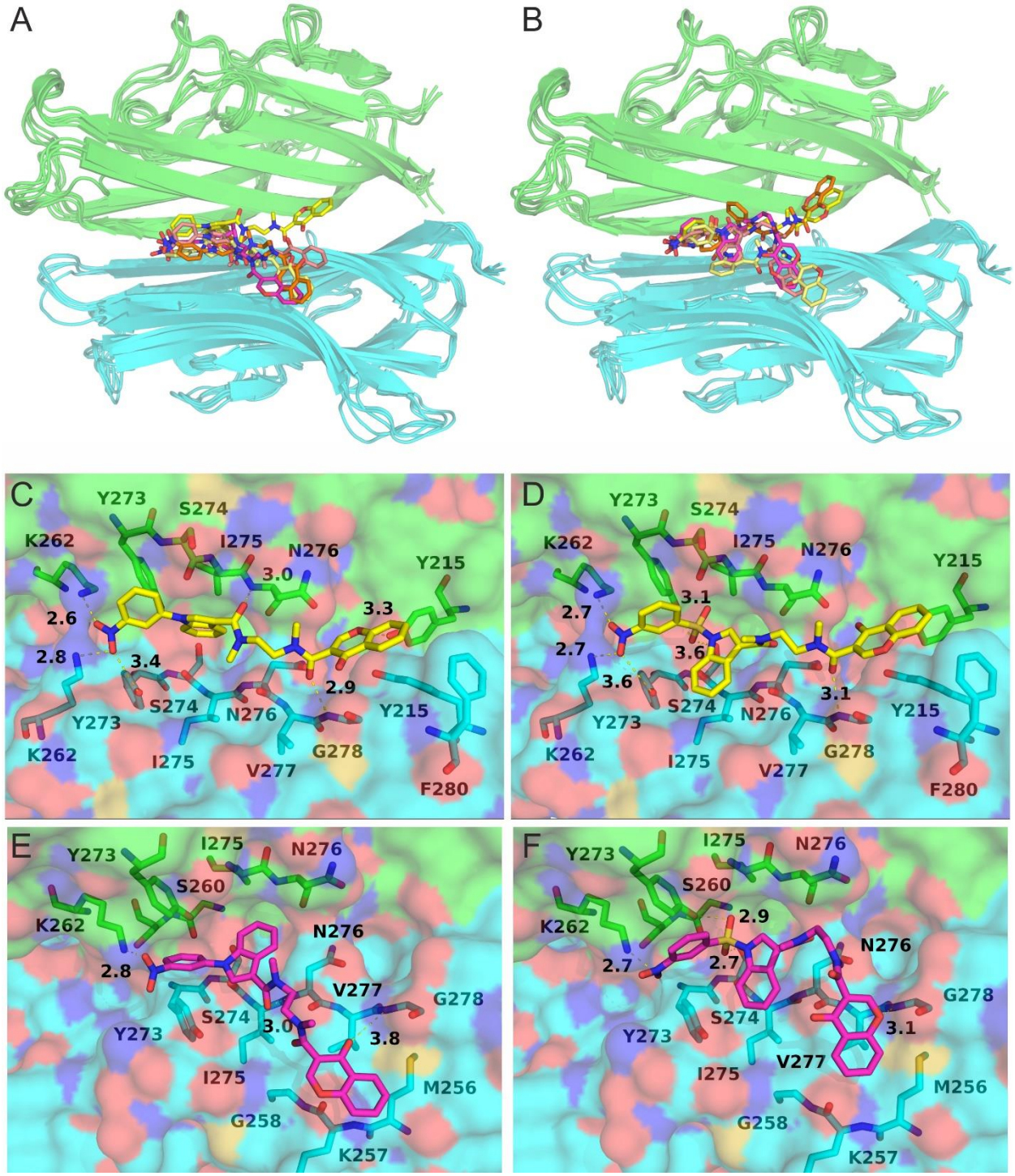

Figure S10. (A, B) Superposition of 5 top-ranked bound poses of **3b** (A) and **4c** (B) in complex with representative models of human RANKL dimer. **(C–F)** Close-up views of the binding interface from the selected models of RANKL-r2 in complex with **3b** (C) and **4c** (D), and of the RANKL-min model in complex with **3b** (E) and **4c** (F).

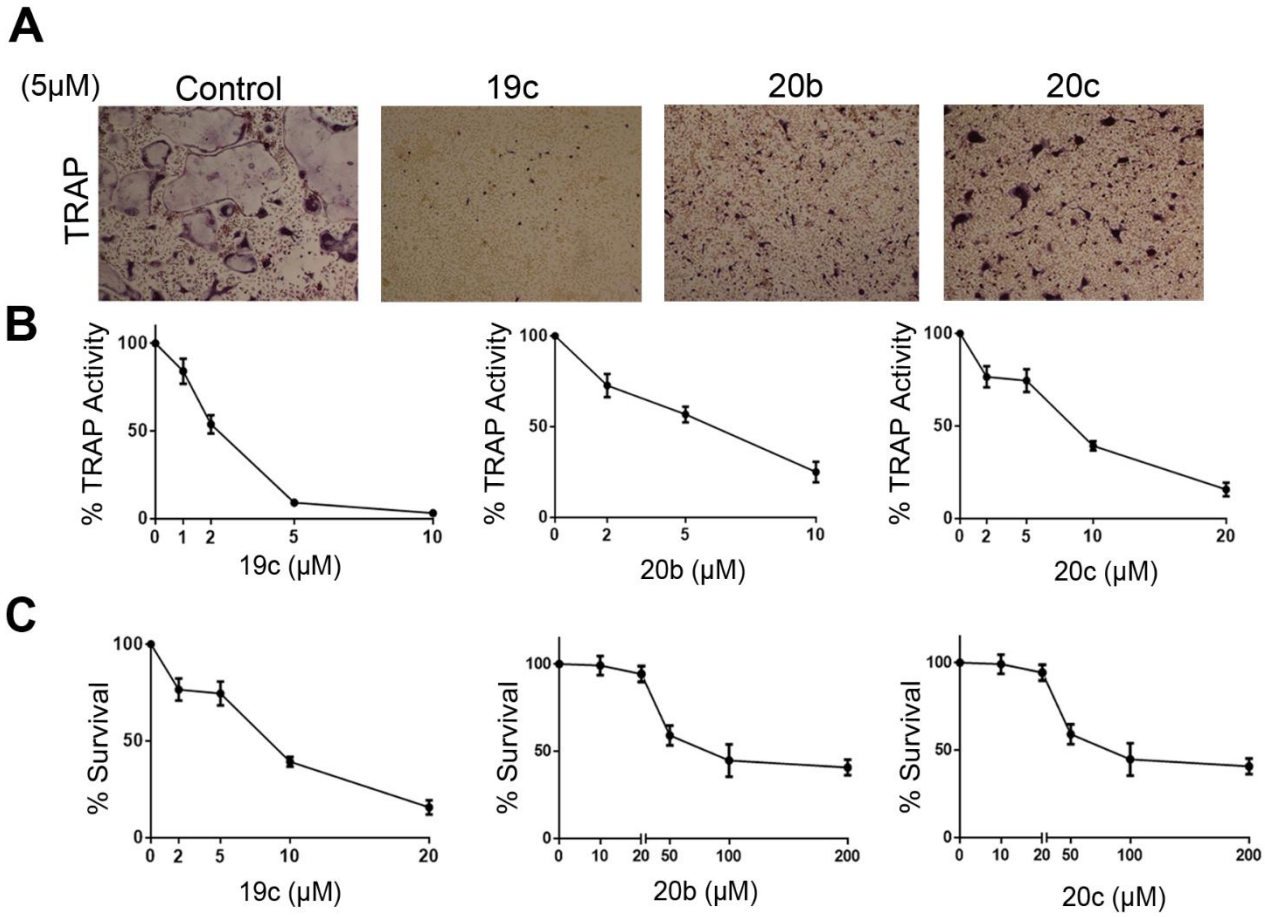

Figure S11. (**A**) Osteoclastogenesis cultures treated with **19c**, **20b** and **20c** at 5 μM in the presence of RANKL (40 ng/mL) and M-CSF (25 ng/mL) for 5 days upon staining with TRAP. (**B**) IC_{50} calculation for each compound based on TRAP activity measured at day 4. (**C**) LC_{50} calculation for each compound on BMM cell viability by MTT assay.

Table S7. Docking results of the 10 top-ranked clusters of conformations obtained for compound **19a** against the 6 representative conformations of the human RANKL dimer model. The lowest and the mean binding energy, along with the number of conformations for each cluster are given.

Cluster Rank	Low. ΔG^{est} (Kcal/mol)	No. Conf.	Mean ΔG^{est} (Kcal/mol)
RANKL-min			
1	**-9.85**	**17**	**-9.04**
2	-8.80	6	-7.94
3	-8.77	4	-8.16
4	-8.60	2	-8.55
5	-8.58	8	-8.00
6	-8.46	1	-8.46
7	-8.27	4	-7.53
8	-8.26	7	-7.64
9	-8.25	2	-8.16
10	-8.19	3	-8.10
RANKL-r1			
1	**-10.01**	**12**	**-9.09**
2	-9.66	8	-9.20
3	-9.27	3	-8.21
4	-9.12	11	-8.26
5	-8.87	2	-8.71
6	-8.84	5	-8.27
7	-8.66	4	-8.18
8	-8.56	2	-8.30
9	-8.55	2	-8.42
10	-8.48	3	-8.03
RANKL-r2			
1	**-10.30**	**12**	**-9.40**
2	-10.11	9	-9.40
3	-9.37	3	-8.82
4	-9.19	1	-9.19
5	-9.06	4	-8.21
6	-8.89	9	-8.52
7	-8.82	3	-8.21
8	-8.67	8	-8.19
9	-8.60	3	-8.22
10	-8.53	3	-8.14

Cluster Rank	Low. ΔG^{est} (Kcal/mol)	No. Conf.	Mean ΔG^{est} (Kcal/mol)
RANKL-c1			
1	-10.91	5	-9.83
2	-10.46	3	-8.99
3	**-9.77**	**21**	**-8.93**
4	-9.60	4	-9.04
5	-9.51	3	-8.98
6	-9.15	1	-9.15
7	-9.10	2	-9.03
8	-8.76	4	-8.29
9	-8.72	3	-8.48
10	-8.70	3	-8.33
RANKL-c2			
1	**-10.49**	**10**	**-9.36**
2	-9.38	8	-8.58
3	-9.25	1	-9.25
4	-9.23	4	-8.58
5	-9.21	3	-8.52
6	-9.14	1	-9.14
7	-9.14	2	-9.11
8	-8.97	5	-8.38
9	-8.96	1	-8.96
10	-8.93	1	-8.93
RANKL-c3			
1	-9.94	1	-9.94
2	-9.60	2	-8.93
3	-9.46	1	-9.46
4	-8.97	2	-8.25
5	**-8.87**	**13**	**-7.87**
6	-8.82	3	-8.17
7	-8.69	5	-7.47
8	-8.61	1	-8.61
9	-8.55	1	-8.55
10	-8.51	2	-8.41

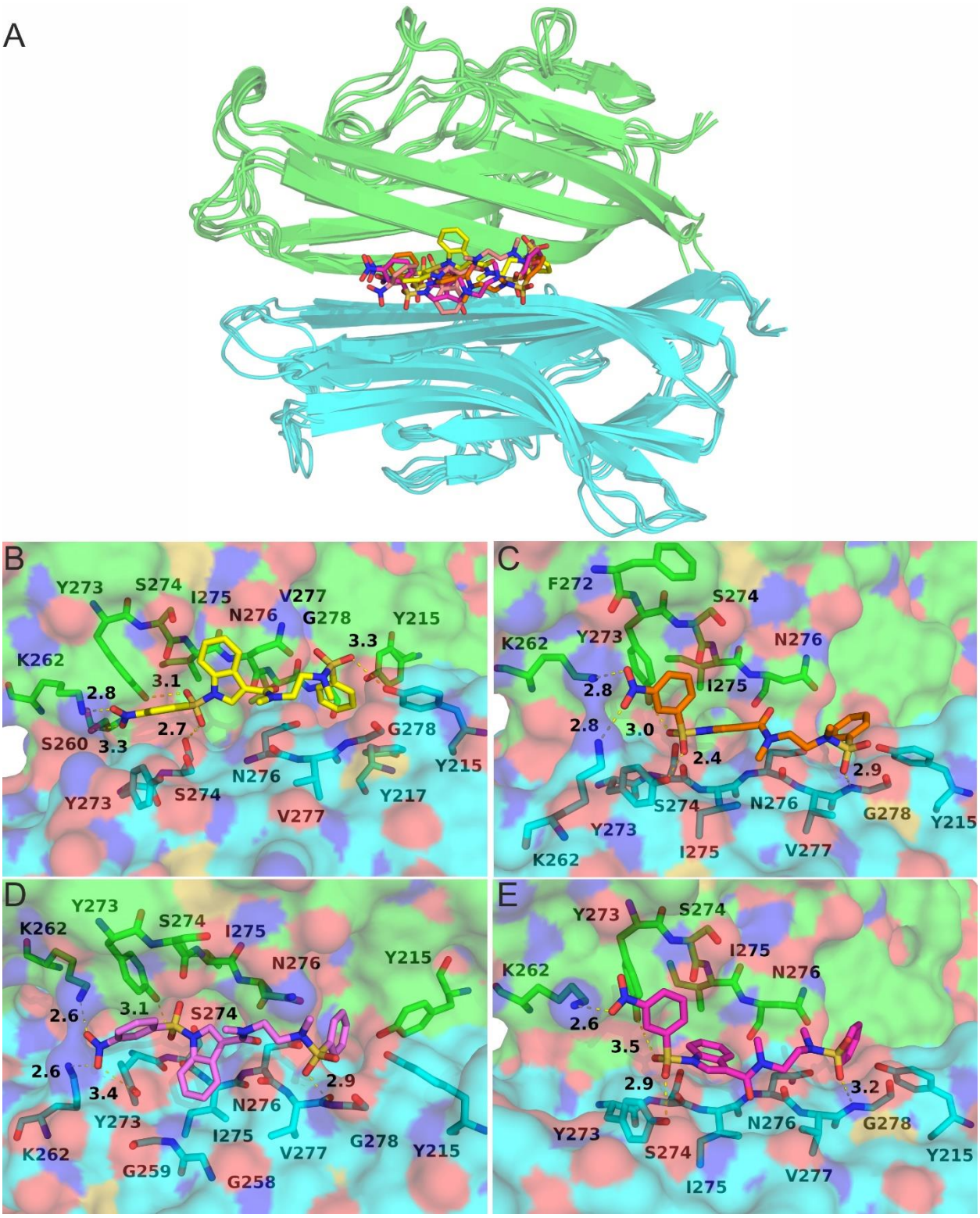

Figure S12. (A) Superposition of 4 similar, top-ranked bound poses of **19a** in complex with representative models of human RANKL dimer. Close-up views of the binding interface from the model of RANKL-min (**B**), RANKL-r2 (**C**), RANKL-c2 (**D**) and RANKL-c3 (**E**) with the corresponding bound pose of compound **19a**.

Table S8. Docking results of the 10 top-ranked clusters of conformations obtained for compound **19b** against the 6 representative conformations of the human RANKL dimer model. The lowest and the mean binding energy, along with the number of conformations for each cluster are given.

Cluster Rank	Low. ΔG^{est} (Kcal/mol)	No. Conf.	Mean ΔG^{est} (Kcal/mol)
RANKL-min			
1	**-10.65**	**10**	**-9.49**
2	-9.45	5	-8.83
3	-9.04	6	-8.16
4	-8.88	2	-8.40
5	-8.56	3	-8.36
6	-8.56	3	-7.90
7	-8.54	2	-7.71
8	-8.53	5	-7.67
9	-8.50	1	-8.50
10	-8.29	2	-7.78
RANKL-r1			
1	-9.92	3	-9.05
2	-9.78	4	-9.01
3	-9.52	2	-9.24
4	-9.43	4	-8.87
5	-9.40	2	-8.86
6	**-9.37**	**6**	**-8.76**
7	-9.28	6	-8.78
8	-9.09	3	-8.31
9	-8.81	2	-8.50
10	-8.60	1	-8.60
RANKL-r2			
1	**-10.33**	**9**	**-9.41**
2	-9.74	3	-9.07
3	-9.69	2	-8.75
4	-9.61	5	-9.04
5	-9.52	3	-9.28
6	-9.49	1	-9.49
7	-9.20	3	-8.99
8	-9.11	2	-8.86
9	-9.08	1	-9.08
10	-9.02	3	-8.73

Cluster Rank	Low. ΔG^{est} (Kcal/mol)	No. Conf.	Mean ΔG^{est} (Kcal/mol)
RANKL-c1			
1	-9.86	1	-9.86
2	-9.73	2	-9.55
3	-9.59	1	-9.59
4	-9.55	2	-8.99
5	-9.45	1	-9.45
6	**-9.43**	**8**	**-8.70**
7	-9.32	2	-8.62
8	-9.26	1	-9.26
9	-9.04	4	-8.53
10	-8.93	3	-8.76
RANKL-c2			
1	-10.50	4	-9.46
2	-10.10	1	-10.10
3	-9.64	2	-8.92
4	-9.60	3	-9.44
5	-9.56	1	-9.56
6	**-9.53**	**10**	**-8.72**
7	-9.52	4	-9.03
8	-9.32	2	-8.69
9	-9.05	1	-9.05
10	-8.99	2	-8.83
RANKL-c3			
1	-9.28	2	-8.98
2	-9.21	4	-8.46
3	-9.21	4	-8.35
4	**-8.97**	**5**	**-7.91**
5	-8.83	2	-8.67
6	-8.74	1	-8.74
7	-8.72	1	-8.72
8	-8.65	1	-8.65
9	-8.52	2	-8.28
10	-8.48	3	-7.93

Table S9. Docking results of the 10 top-ranked clusters of conformations obtained for compound **20a** against the 6 representative conformations of the human RANKL dimer model. The lowest and the mean binding energy, along with the number of conformations for each cluster are given.

Cluster Rank	Low. ΔG^{est} (Kcal/mol)	No. Conf.	Mean ΔG^{est} (Kcal/mol)
RANKL-min			
1	**-10.50**	**50**	**-9.54**
2	-9.54	8	-9.14
3	-9.03	1	-9.03
4	-8.87	6	-8.46
5	-8.62	6	-8.50
6	-8.54	5	-8.34
7	-8.38	3	-8.13
8	-8.36	2	-8.36
9	-8.28	1	-8.28
10	-8.27	1	-8.27
RANKL-r1			
1	-10.21	1	-10.21
2	-9.81	2	-9.31
3	-9.66	10	-9.11
4	-9.57	4	-8.91
5	-9.50	3	-9.06
6	-9.45	4	-9.25
7	-9.22	6	-8.96
8	**-9.21**	**18**	**-8.98**
9	-9.17	7	-8.84
10	-9.01	1	-9.01
RANKL-r2			
1	**-10.61**	**31**	**-9.65**
2	-10.36	9	-9.67
3	-9.95	9	-9.35
4	-9.46	3	-9.38
5	-9.46	13	-9.25
6	-9.44	1	-9.44
7	-9.41	4	-9.30
8	-9.18	10	-8.72
9	-9.16	4	-9.07
10	-9.14	3	-8.56

Cluster Rank	Low. ΔG^{est} (Kcal/mol)	No. Conf.	Mean ΔG^{est} (Kcal/mol)
RANKL-c1			
1	-11.09	10	-10.68
2	-10.97	8	-10.43
3	-10.77	6	-9.96
4	-10.65	13	-9.96
5	-9.94	4	-9.62
6	-9.94	12	-9.54
7	-9.80	4	-9.71
8	-9.62	2	-9.05
9	**-9.54**	**16**	**-9.38**
10	-9.46	5	-9.06
RANKL-c2			
1	-10.20	10	-9.64
2	-10.00	1	-10.00
3	-9.81	7	-9.52
4	**-9.78**	**14**	**-9.40**
5	-9.75	6	-9.06
6	-9.74	8	-9.42
7	-9.73	11	-9.48
8	-9.59	1	-9.59
9	-9.58	4	-9.37
10	-9.55	4	-9.22
RANKL-c3			
1	-10.52	3	-10.09
2	-10.09	4	-9.47
3	**-9.84**	**8**	**-9.30**
4	-9.83	7	-9.51
5	-9.50	1	-9.50
6	-9.43	7	-8.67
7	-9.40	3	-8.91
8	-9.33	1	-9.33
9	-9.31	6	-9.01
10	-8.89	2	-8.80

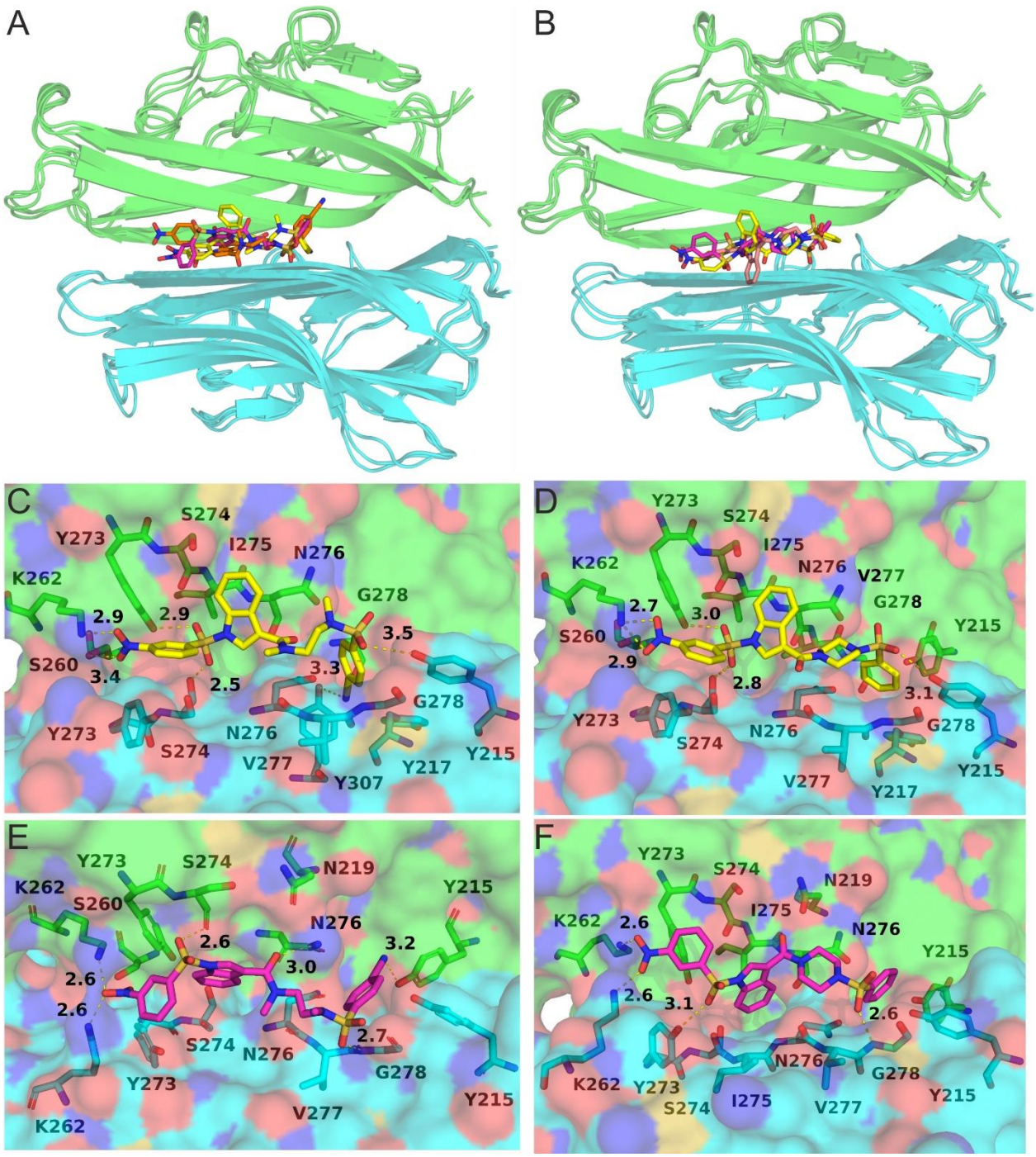

Figure S13. (A, B) Superposition of 3 top-ranked bound poses of **19b** (A) and **20a** (B) in complex with representative models of human RANKL dimer. (C, D) Close-up views of the binding interface from the selected models of RANKL-min in complex with **19b** and **20a**, respectively. (E) Close-up view of highly populated model of **19b** in complex with RANKL-c2 model. (F) Close-up view of the second highest-populated, top-ranked bound pose of **20a** in complex with RANKL-r2 representative model.

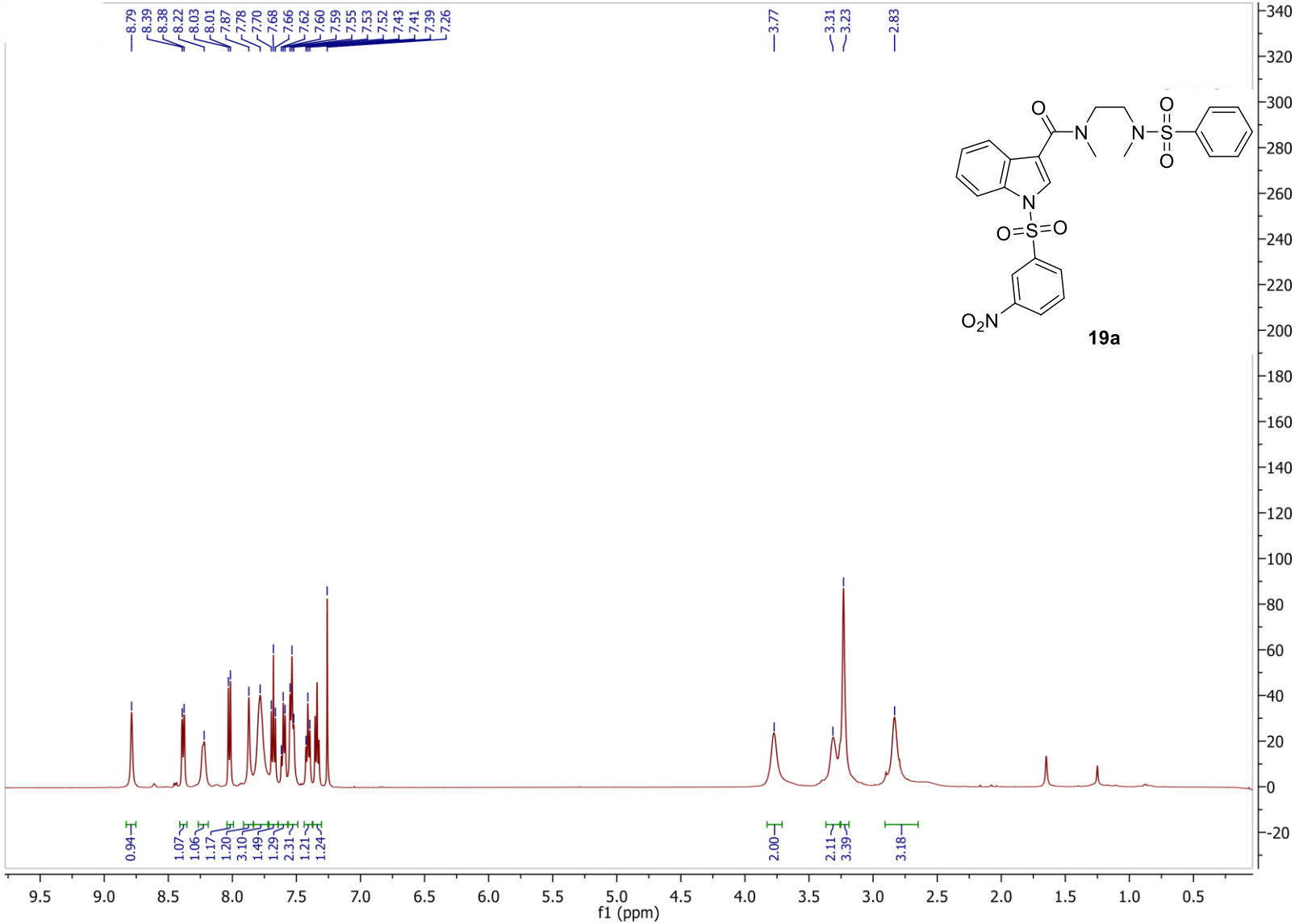

Figure S14 (a). ^{1}H NMR (500 MHz, $CDCl_3$) spectrum of **19a.**

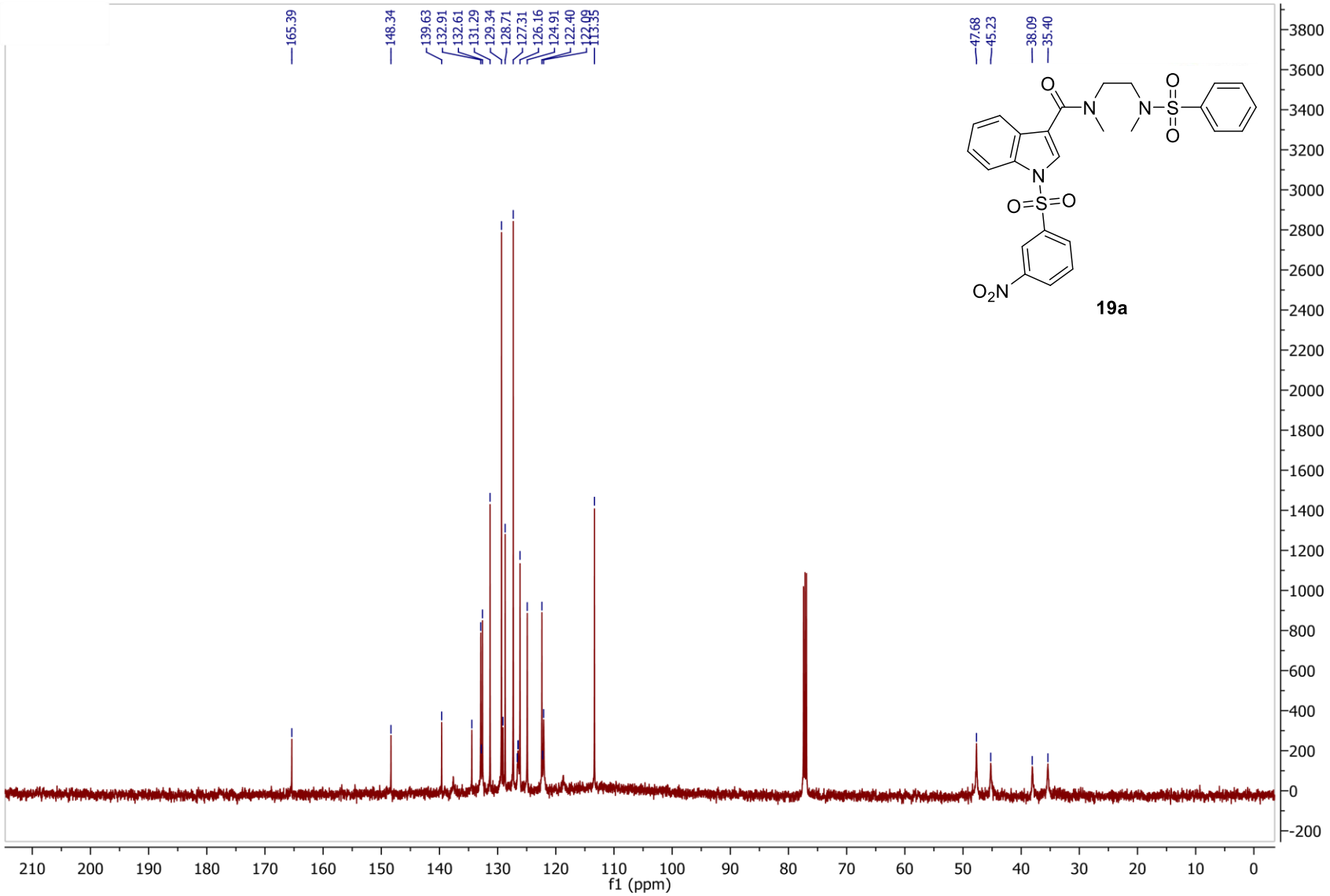

Figure S14 (b). ^{13}C NMR (125.7 MHz, $CDCl_3$) spectrum of **19a.**

==== Shimadzu LCMSsolution Analysis Report ====

Purospher_RP8
Sample Name : 97_101
Analysis Request :97_101_1
Data File Name : 97_101_1.lcd
Method File Name : ESI_grad_MeOH-aqCH3COONH4 10mM pH=3.9 formic.lcm
Data Acquired : 16/10/2014 5:40:01 μμ
Data Processed : 16/10/2014 6:25:16 μμ

Method

Column: Purospher C8, 25x4.6, 5um
Mobile Phase A: aq. CH3COONH4 10mM, pH=3.9 with formic acid
Mobile Phase B: MeOH
% Pump B Concetrate: 80.0
Flow (ml/min): 0.5000

Oven Temp.: 30
Detector A:SPD-20A
UV_1.Wavelength: 225
UV_2.Wavelength: 254
LC Program

Time	Unit	Command	Value
0.01	Pumps	B.Conc	80
20.00	Pumps	B.Conc	100
35.00	Pumps	B.Conc	100
35.01	Pumps	B.Conc	80
45.00	Pumps	B.Conc	80
45.01	Controller	Stop	

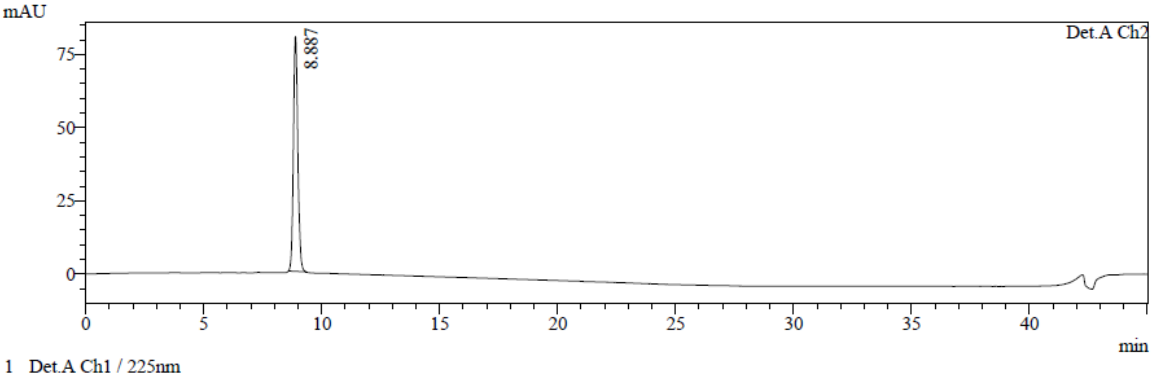

1 Det.A Ch1 / 225nm
2 Det.A Ch2 / 254nm

PeakTable

Detector A Ch1 225nm

Peak#	Ret. Time	Area	Height	Area %	Height %
1	8.885	1645339	125630	100.000	100.000
Total		1645339	125630	100.000	100.000

PeakTable

Detector A Ch2 254nm

Peak#	Ret. Time	Area	Height	Area %	Height %
1	8.887	1044686	80355	100.000	100.000
Total		1044686	80355	100.000	100.000

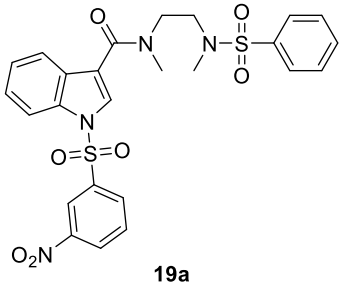

19a

MS Spectrum Graph

#:1 Ret.Time:Averaged 8.250-9.625(Scan#:901-1051)
BG Mode:Averaged 30.690-44.249(3349-4829)
Mass Peaks:416 Base Peak:557.35(223296) Polarity:Pos Segment1 - Event1

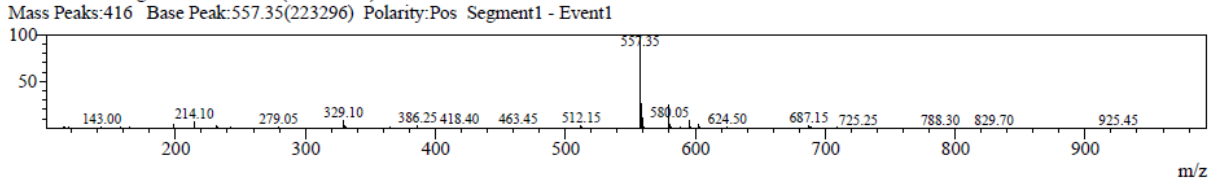

Figure S14 (c). LC-MS analysis of **19a**.

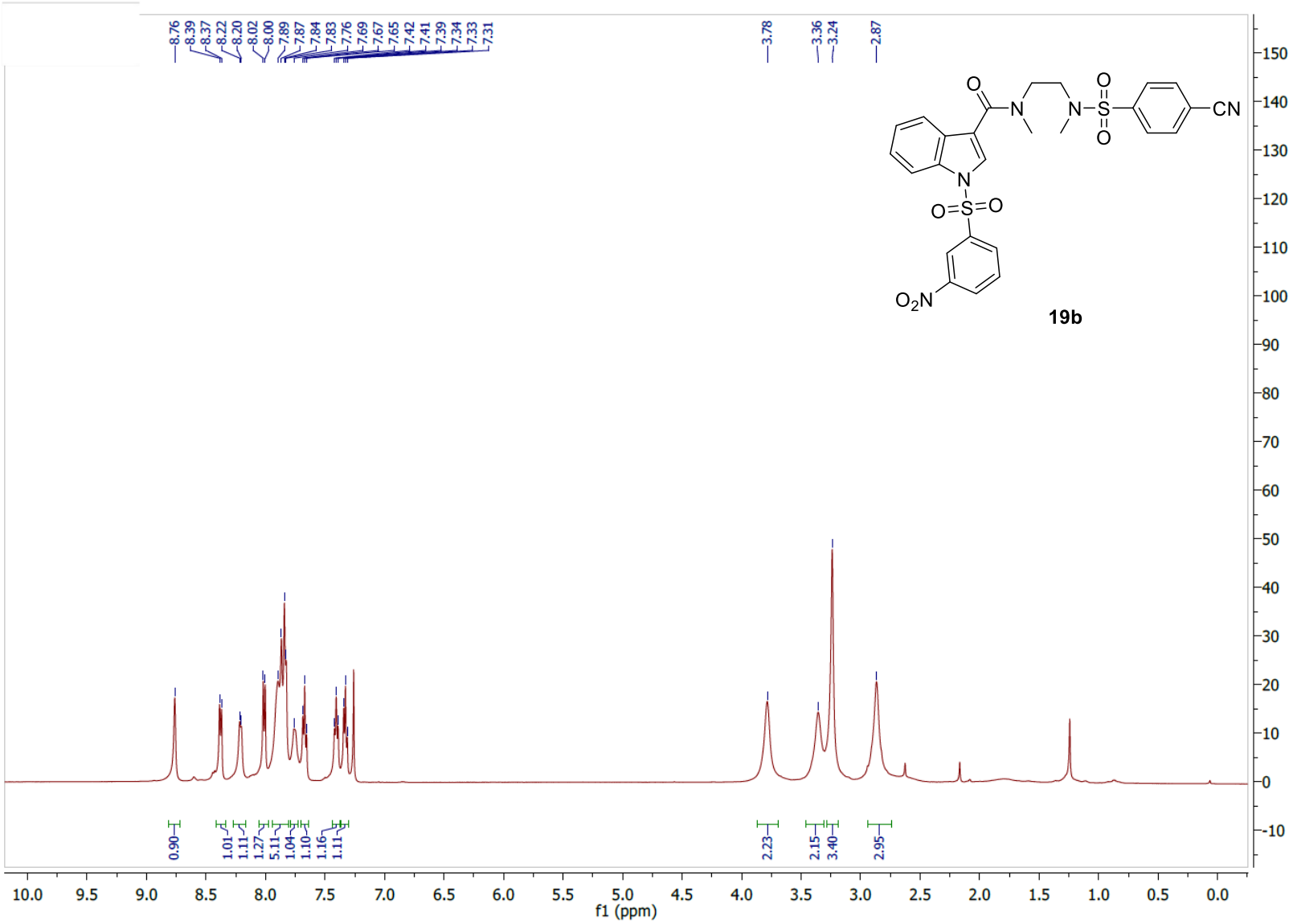

Figure S15 (a). ^{1}H NMR (500 MHz, $CDCl_3$) spectrum of **19b**.

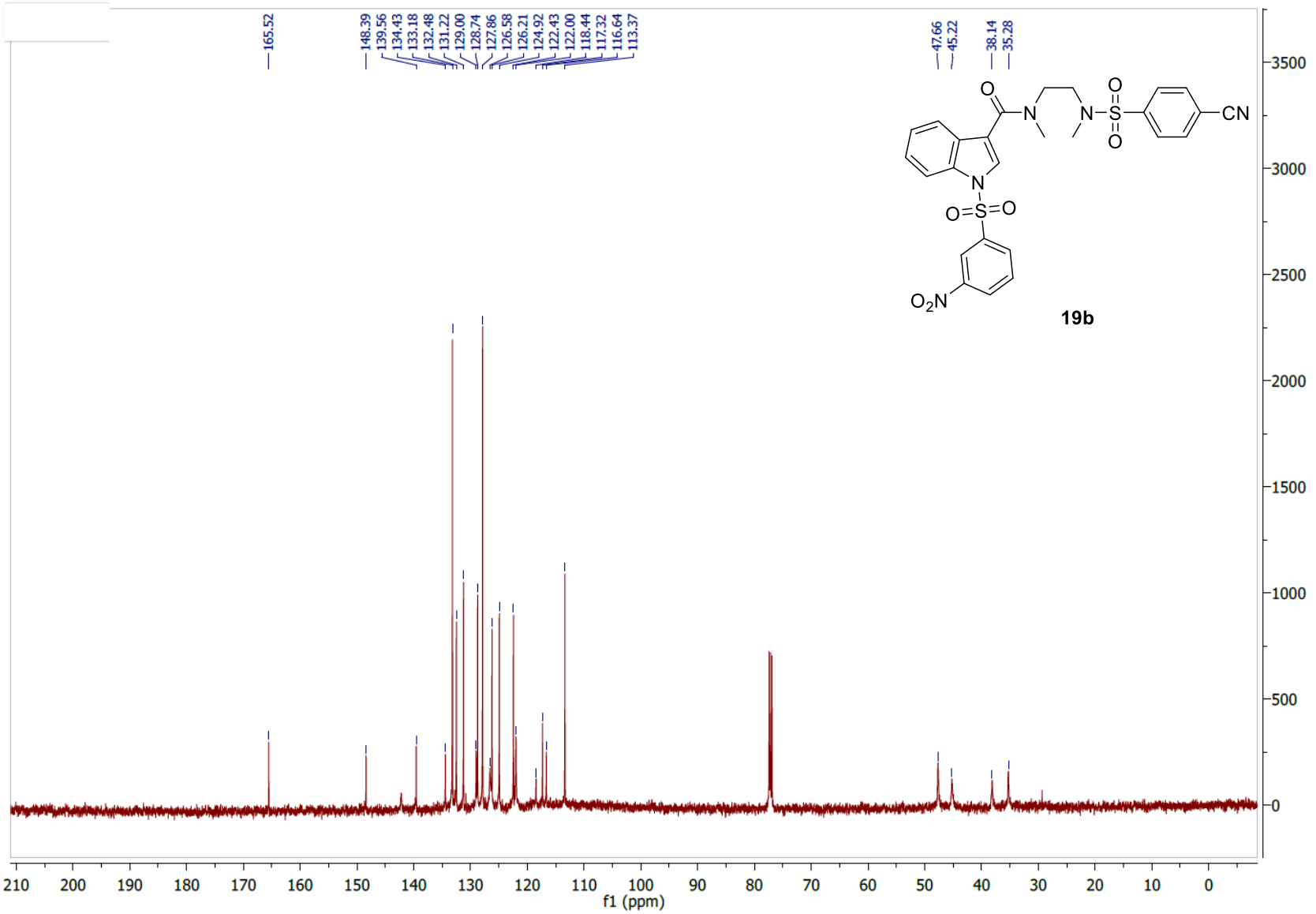

Figure S15 (b). ^{13}C NMR (125.7 MHz, $CDCl_3$) spectrum of **19b**.

==== Shimadzu LCMSsolution Analysis Report ====

Purospher_RP8
Sample Name : 98_102
Analysis Request :98_102_1
Data File Name : 98_102_1.lcd
Method File Name : ESI_grad_MeOH-aqCH3COONH4 10mM pH=3.9 formic.lcm
Data Acquired : 16/10/2014 6:25:44 μμ
Data Processed : 16/10/2014 7:10:51 μμ

Method

Column: Purospher C8, 25x4.6, 5um
Mobile Phase A: aq. CH3COONH4 10mM, pH=3.9 with formic acid
Mobile Phase B: MeOH
% Pump B Concetrate: 80.0
Flow (ml/min): 0.5000

Oven Temp.: 30
Detector A:SPD-20A
UV_1.Wavelength: 225
UV_2.Wavelength: 254
LC Program

Time	Unit	Command	Value
0.01	Pumps	B.Conc	80
20.00	Pumps	B.Conc	100
35.00	Pumps	B.Conc	100
35.01	Pumps	B.Conc	80
45.00	Pumps	B.Conc	80
45.01	Controller	Stop	

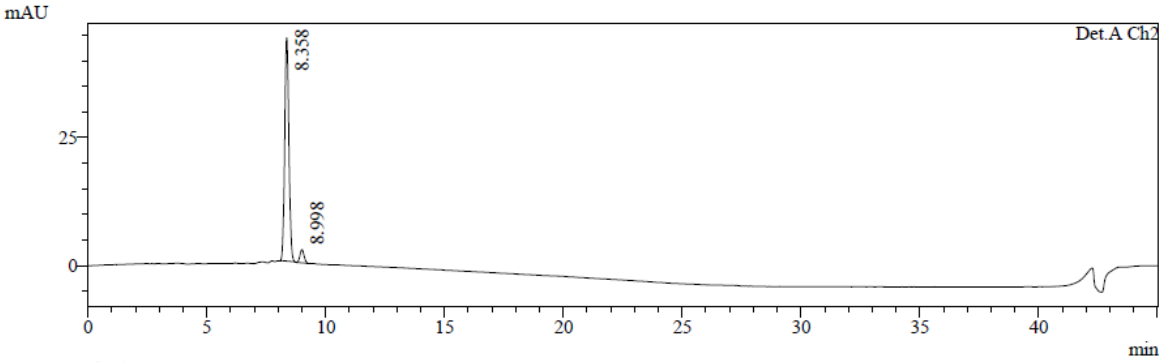

1 Det.A Ch1 / 225nm
2 Det.A Ch2 / 254nm

PeakTable

Detector A Ch1 225nm

Peak#	Ret. Time	Area	Height	Area %	Height %
1	8.356	637661	52052	95.695	95.009
2	8.986	28685	2734	4.305	4.991
Total		666346	54787	100.000	100.000

PeakTable

Detector A Ch2 254nm

Peak#	Ret. Time	Area	Height	Area %	Height %
1	8.358	533505	43612	94.630	94.447
2	8.998	30274	2564	5.370	5.553
Total		563779	46176	100.000	100.000

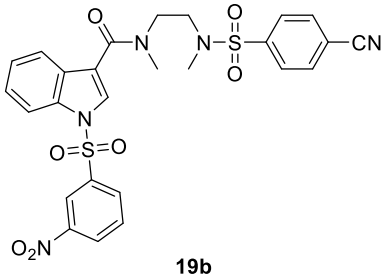

19b

MS Spectrum Graph

#:1 Ret.Time:Averaged 7.828-8.782(Scan#:855-959)
BG Mode:Averaged 33.128-43.190(3615-4713)
Mass Peaks:366 Base Peak:582.20(95313) Polarity:Pos Segment1 - Event1

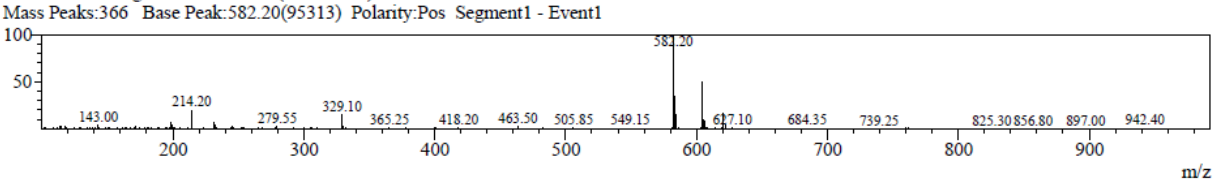

Figure S15 (c). LC-MS analysis of **19b**.

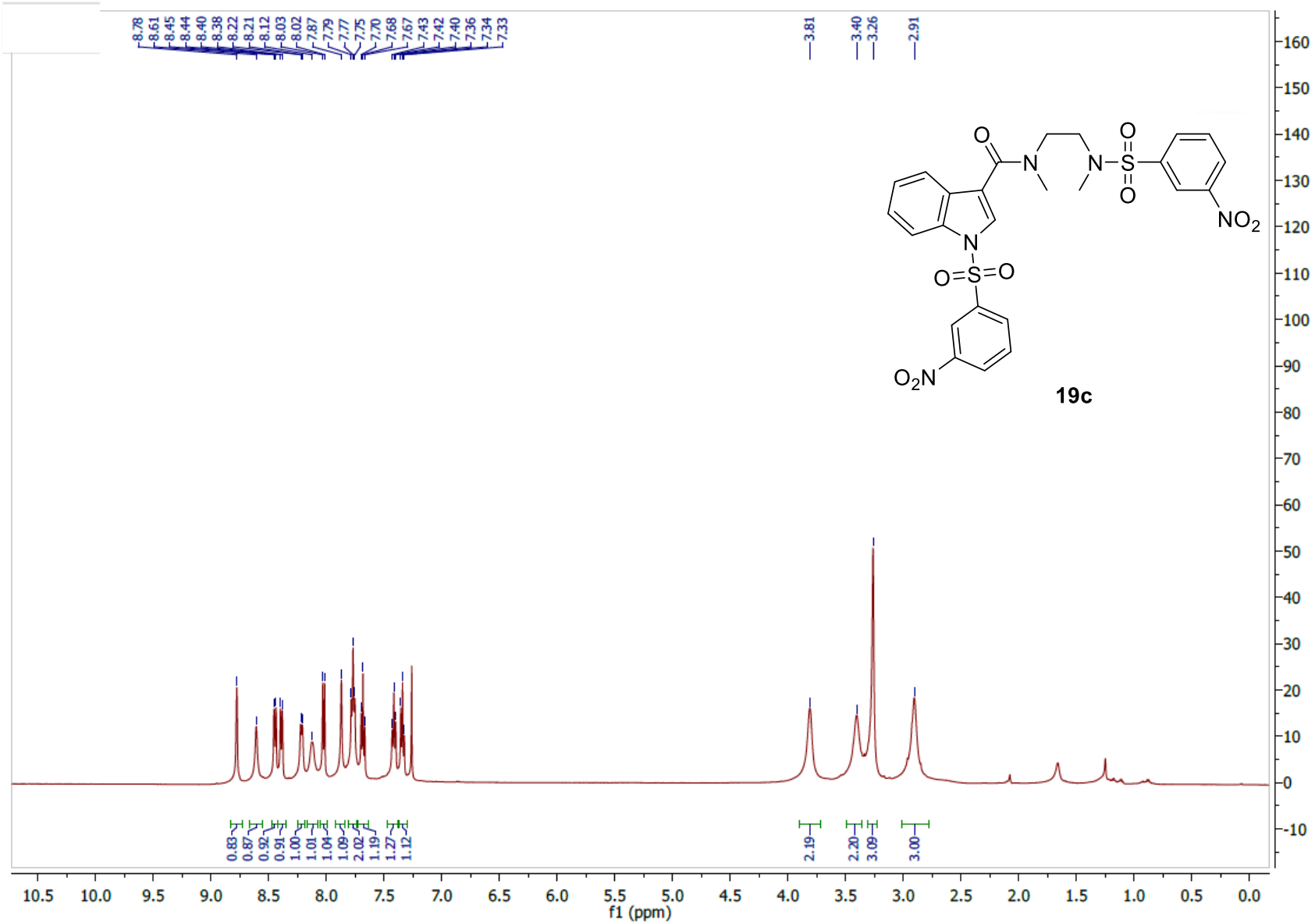

Figure S16 (a). ^{1}H NMR (500 MHz, $CDCl_3$) spectrum of **19c**.

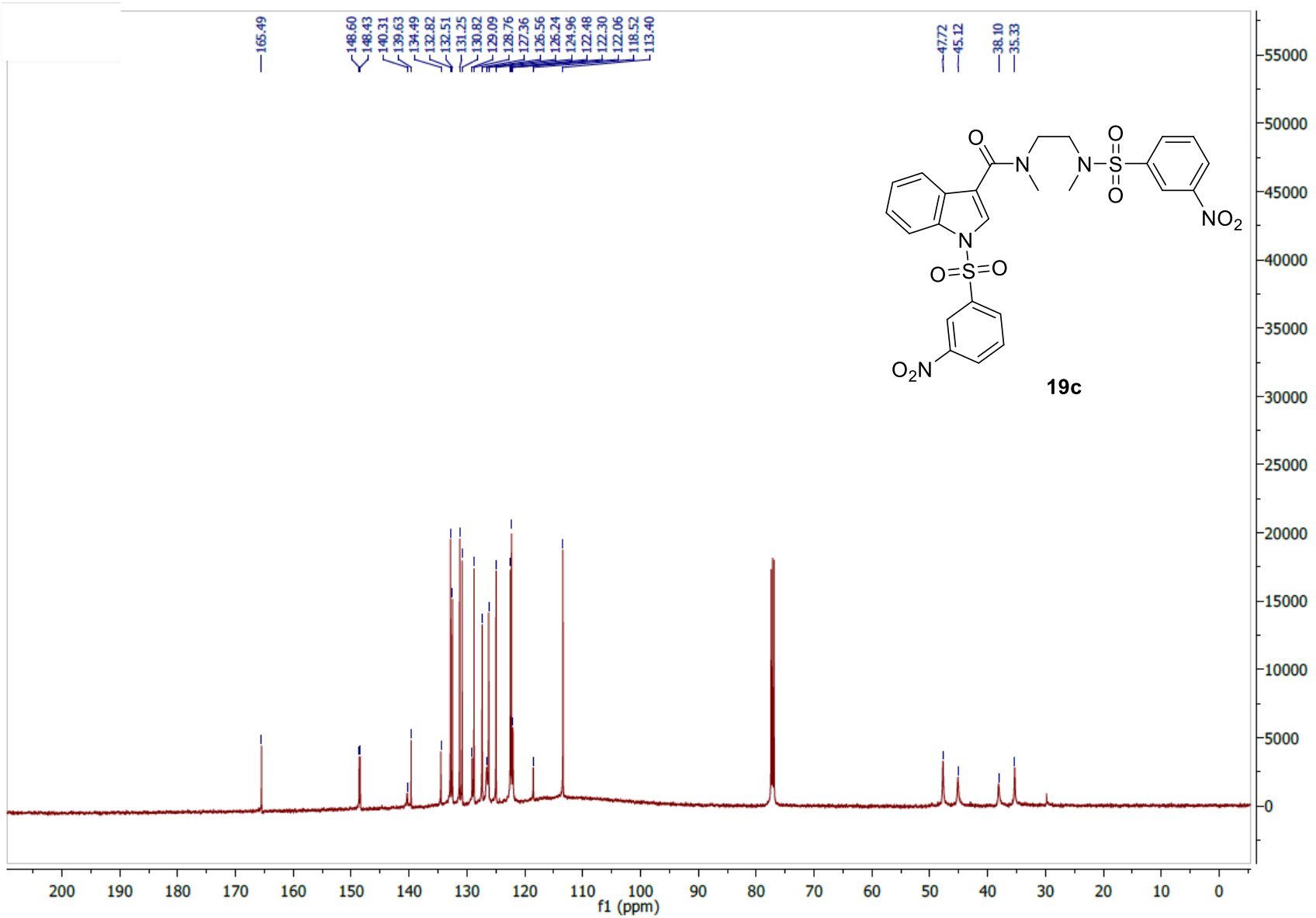

Figure S16 (b). ^{13}C NMR (125.7 MHz, $CDCl_3$) spectrum of **19c**.

==== Shimadzu LCMSsolution Analysis Report ====

Purospher_RP8
Sample Name : 103_107
Analysis Request :103_107_1
Data File Name : 103_107_1.lcd
Method File Name : ESI_grad_MeOH-aqCH3COONH4 10mM pH=3.9 formic.lcm
Data Acquired : 16/10/2014 8:42:45 μμ
Data Processed : 17/10/2014 1:57:50 μμ

Method

Column: Purospher C8, 25x4.6, 5um
Mobile Phase A: aq. CH3COONH4 10mM, pH=3.9 with formic acid
Mobile Phase B: MeOH
% Pump B Concetrate: 80.0
Flow (ml/min): 0.5000

Oven Temp.: 30
Detector A:SPD-20A
UV_1.Wavelength: 225
UV_2.Wavelength: 254
LC Program

Time	Unit	Command	Value
0.01	Pumps	B.Conc	80
20.00	Pumps	B.Conc	100
35.00	Pumps	B.Conc	100
35.01	Pumps	B.Conc	80
45.00	Pumps	B.Conc	80
45.01	Controller	Stop	

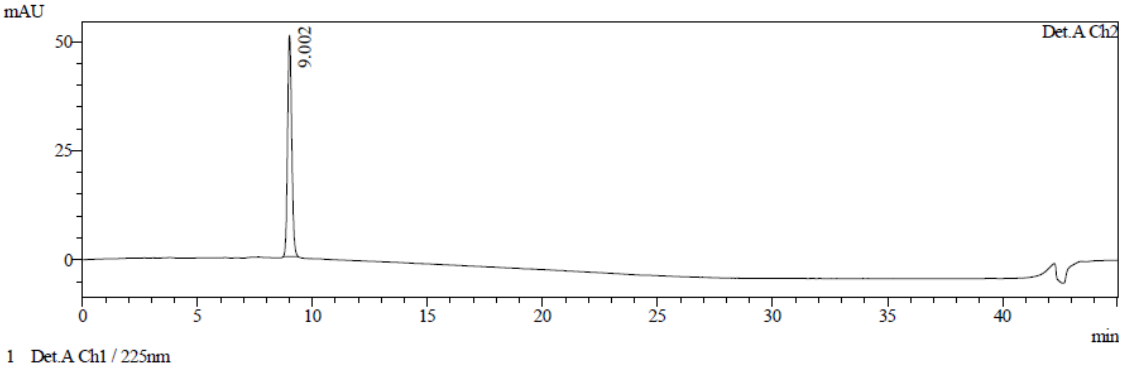

1 Det.A Ch1 / 225nm
2 Det.A Ch2 / 254nm

PeakTable

Detector A Ch1 225nm

Peak#	Ret. Time	Area	Height	Area %	Height %
1	9.001	836063	66098	100.000	100.000
Total		836063	66098	100.000	100.000

PeakTable

Detector A Ch2 254nm

Peak#	Ret. Time	Area	Height	Area %	Height %
1	9.002	633694	50685	100.000	100.000
Total		633694	50685	100.000	100.000

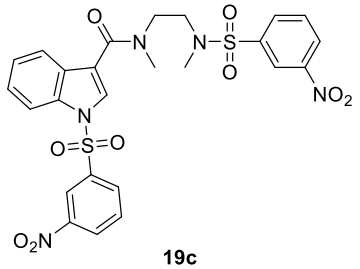

19c

MS Spectrum Graph

#:1 Ret.Time:Averaged 8.360-9.533(Scan#:913-1041)
BG Mode:Averaged 30.268-43.085(3303-4701)
Mass Peaks:408 Base Peak:602.25(100930) Polarity:Pos Segment1 - Event1

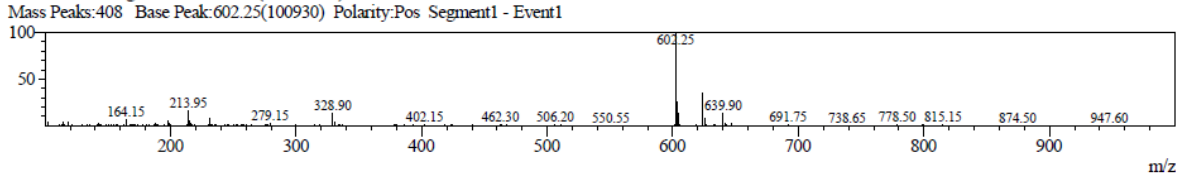

Figure S16 (c). LC-MS analysis of **19c**.

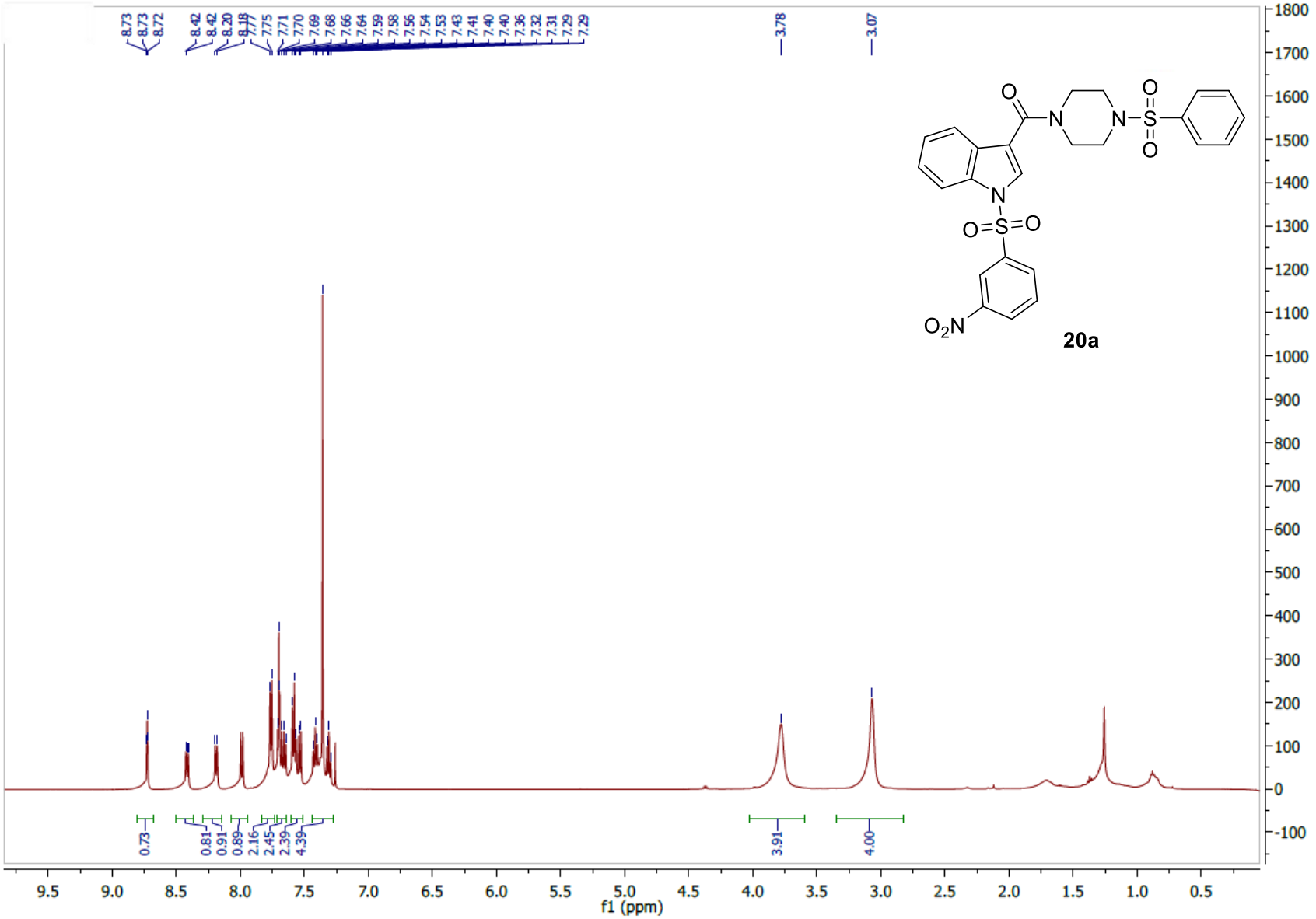

Figure S17 (a). ^{1}H NMR (500 MHz, $CDCl_3$) spectrum of **20a**.

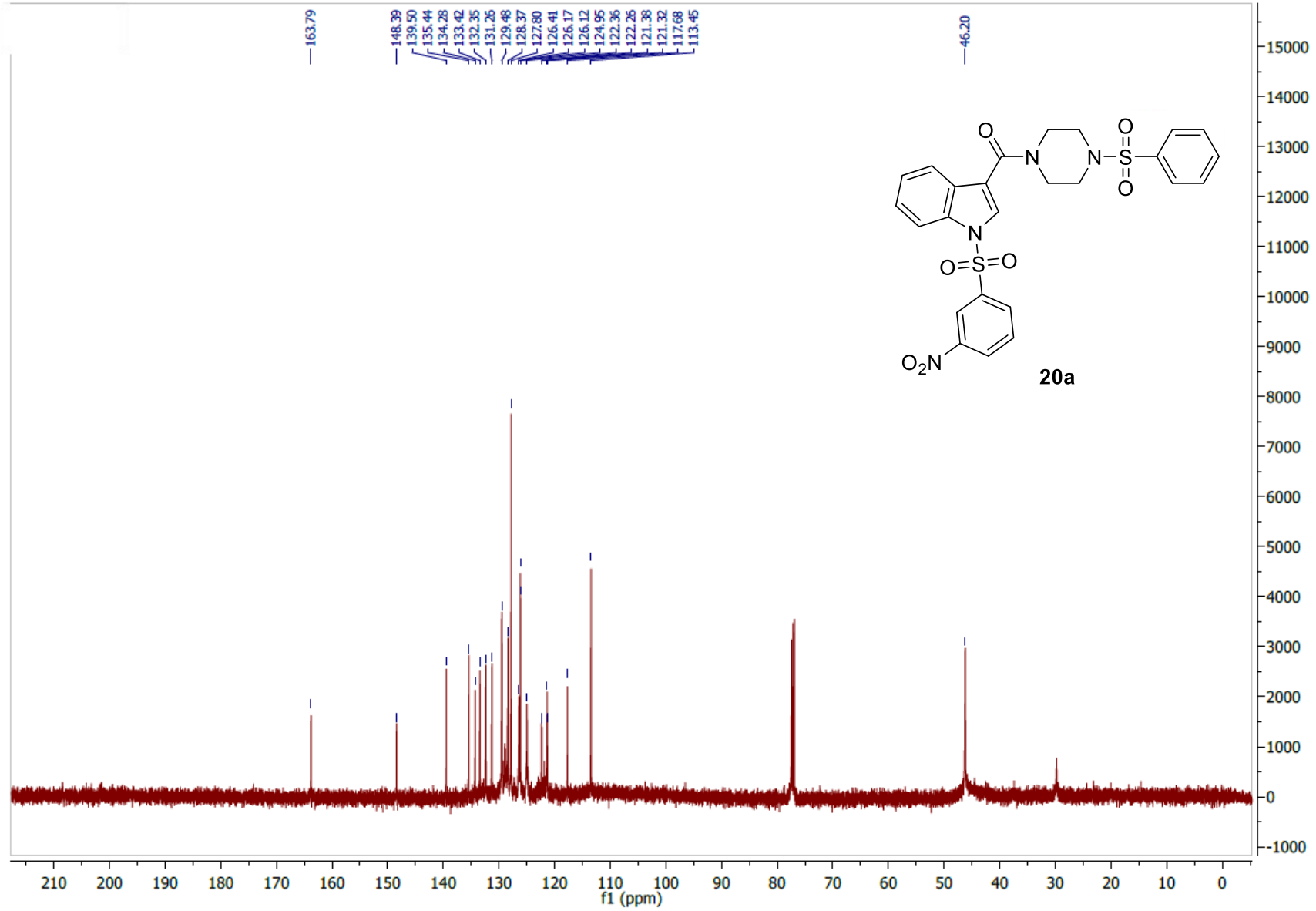

Figure S17 (b). ^{13}C NMR (125.7 MHz, $CDCl_3$) spectrum of **20a**.

==== Shimadzu LCMSsolution Analysis Report ====

Purospher_RP8
Sample Name : 78_81
Analysis Request :78_81_4
Data File Name : 78_81_4.lcd
Method File Name : ESI_grad_MeOH-aqCH3COONH4 10mM pH=3.9 formic.lcm
Data Acquired : 22/9/2014 5:49:11 μμ
Data Processed : 22/9/2014 6:34:22 μμ

Method

Column: Purospher C8, 25x4.6, 5um
Mobile Phase A: aq. CH3COONH4 10mM, pH=3.9 with formic acid
Mobile Phase B: MeOH
% Pump B Concetrate: 80.0
Flow (ml/min): 0.5000

Oven Temp.: 30
Detector A:SPD-20A
UV_1.Wavelength: 225
UV_2.Wavelength: 254
LC Program

Time	Unit	Command	Value
0.01	Pumps	B.Conc	80
20.00	Pumps	B.Conc	100
35.00	Pumps	B.Conc	100
35.01	Pumps	B.Conc	80
45.00	Pumps	B.Conc	80
45.01	Controller	Stop	

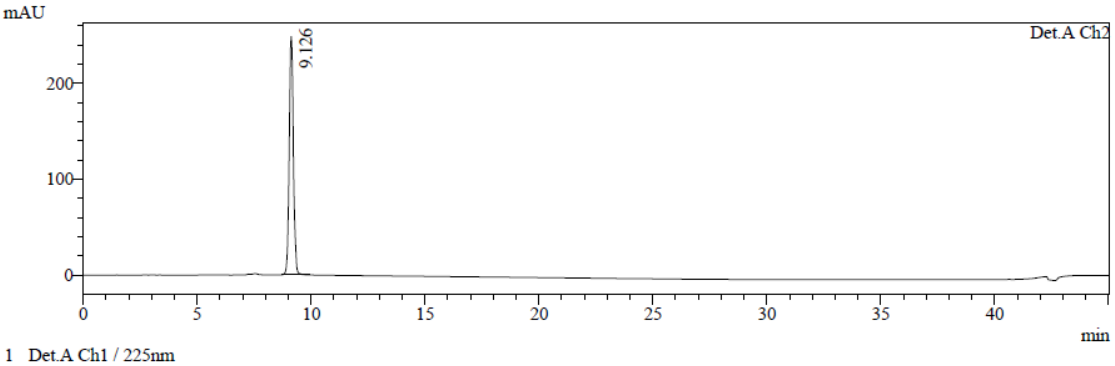

1 Det.A Ch1 / 225nm
2 Det.A Ch2 / 254nm

PeakTable

Detector A Ch1 225nm

Peak#	Ret. Time	Area	Height	Area %	Height %
1	9.125	5144461	404099	99.817	99.758
2	27.269	9421	978	0.183	0.242
Total		5153882	405077	100.000	100.000

PeakTable

Detector A Ch2 254nm

Peak#	Ret. Time	Area	Height	Area %	Height %
1	9.126	3150712	248201	100.000	100.000
Total		3150712	248201	100.000	100.000

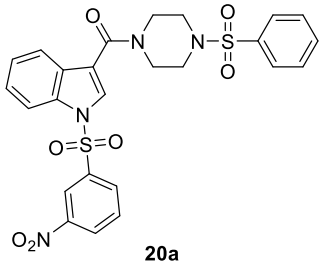

20a

MS Spectrum Graph

#:1 Ret.Time:Averaged 8.672-9.845(Scan#:947-1075)
BG Mode:Averaged 29.957-44.355(3269-4839)
Mass Peaks:430 Base Peak:555.35(184546) Polarity:Pos Segment1 - Event1

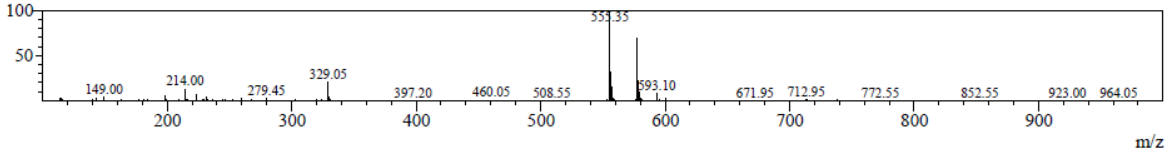

Figure S17 (c). LC-MS analysis of **20a**.

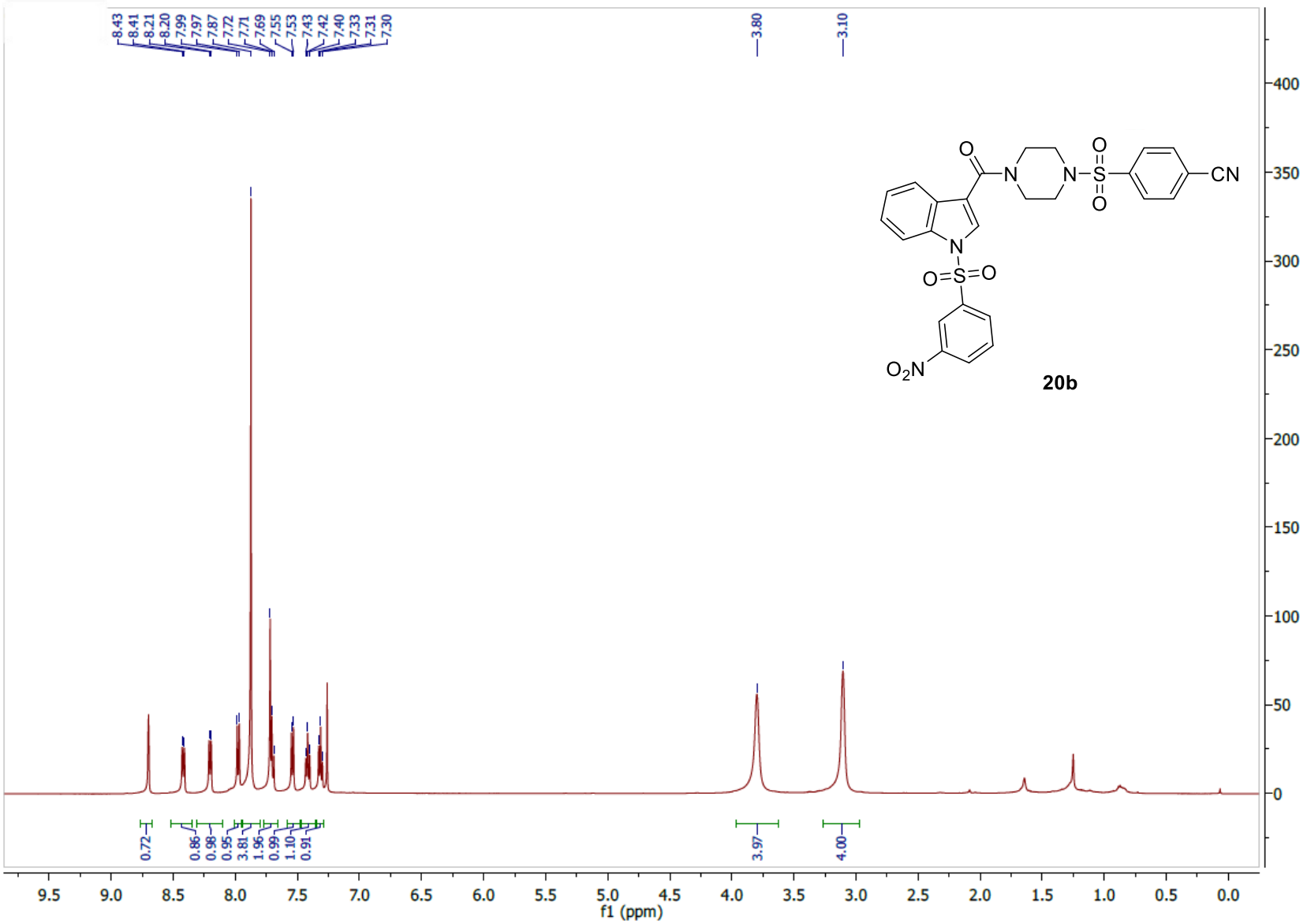

Figure S18 (a). ^{1}H NMR (500 MHz, $CDCl_3$) spectrum of **20b**.

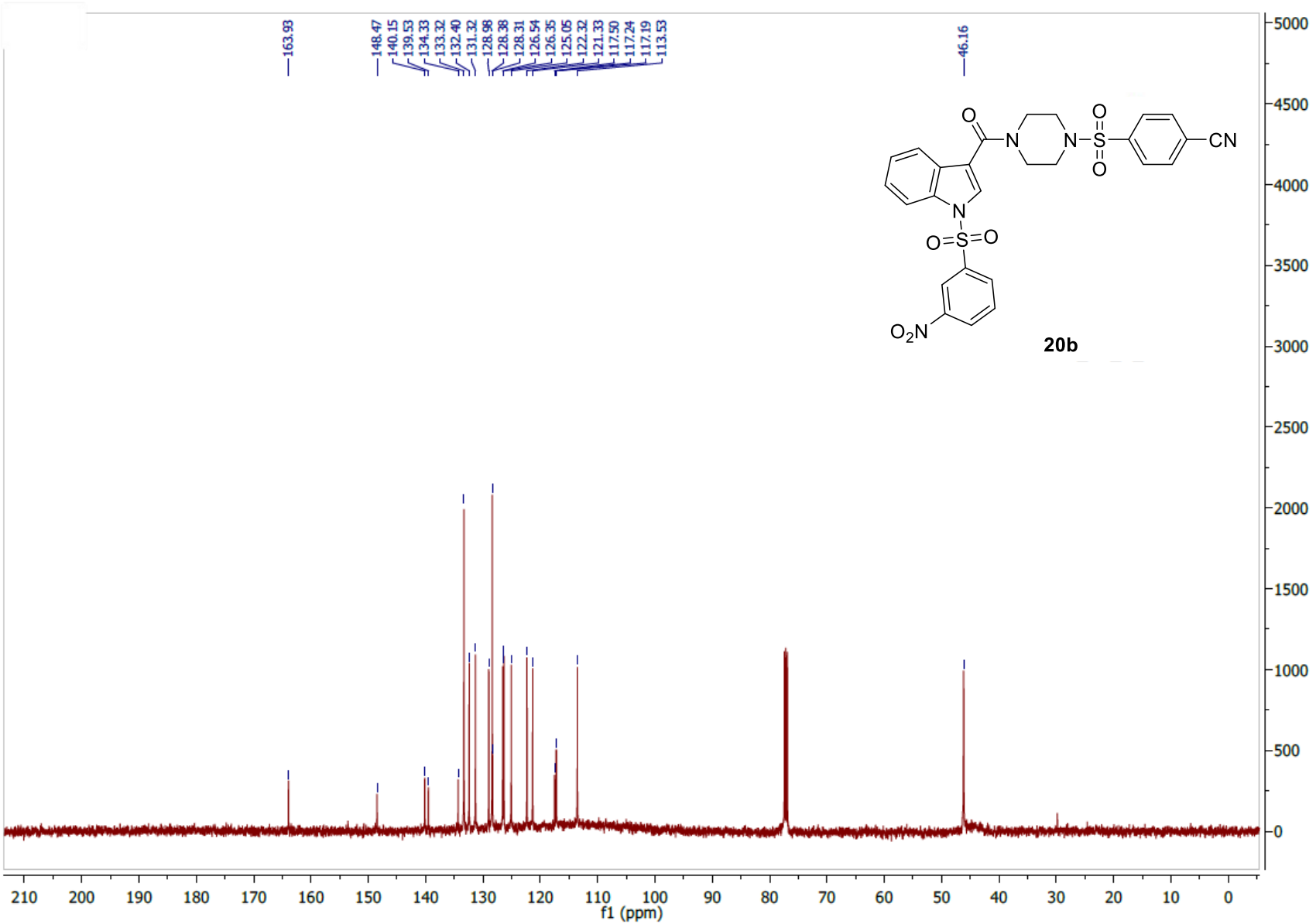

Figure S18 (b). ^{13}C NMR (125.7 MHz, $CDCl_3$) spectrum of **20b**.

==== Shimadzu LCMSsolution Analysis Report ====

Purospher_RP8
Sample Name : 90_93
Analysis Request :90_93_3
Data File Name : 90_93_3.lcd
Method File Name : ESI_grad_MeOH-aqCH3COONH4 10mM pH=3.9 formic.lcm
Data Acquired : 23/9/2014 12:40:19 πμ
Data Processed : 23/9/2014 1:25:28 πμ

Method

Column: Purospher C8, 25x4.6, 5um
Mobile Phase A: aq. CH3COONH4 10mM, pH=3.9 with formic acid
Mobile Phase B: MeOH
% Pump B Concetrate: 80.0
Flow (ml/min): 0.5000

Oven Temp.: 30
Detector A:SPD-20A
UV_1.Wavelength: 225
UV_2.Wavelength: 254
LC Program

Time	Unit	Command	Value
0.01	Pumps	B.Conc	80
20.00	Pumps	B.Conc	100
35.00	Pumps	B.Conc	100
35.01	Pumps	B.Conc	80
45.00	Pumps	B.Conc	80
45.01	Controller	Stop	

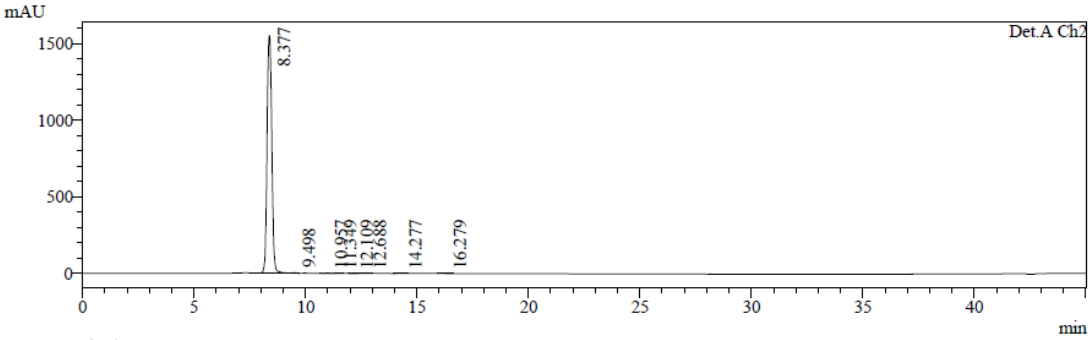

1 Det.A Ch1 / 225nm
2 Det.A Ch2 / 254nm

PeakTable

Detector A Ch1 225nm

Peak#	Ret. Time	Area	Height	Area %	Height %
1	8.377	26373512	1652405	99.672	99.504
2	9.494	86864	8241	0.328	0.496
Total		26460377	1660646	100.000	100.000

PeakTable

Detector A Ch2 254nm

Peak#	Ret. Time	Area	Height	Area %	Height %
1	8.377	22916452	1552823	99.642	99.598
2	9.498	32169	3217	0.140	0.206
3	10.957	20310	962	0.088	0.062
4	11.349	4876	328	0.021	0.021
5	12.109	2451	168	0.011	0.011
6	12.688	7131	581	0.031	0.037
7	14.277	8835	615	0.038	0.039
8	16.279	6533	398	0.028	0.026
Total		22998757	1559093	100.000	100.000

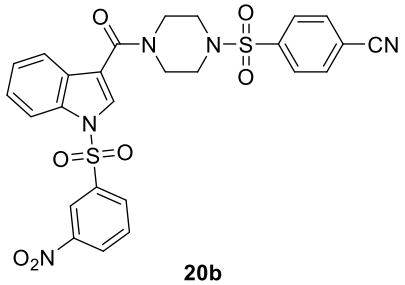

20b

MS Spectrum Graph

#:1 Ret.Time:Averaged 8.048-9.112(Scan#:879-995)
BG Mode:Averaged 30.268-43.402(3303-4735)
Mass Peaks:457 Base Peak:580.05(175534) Polarity:Pos Segment1 - Event1

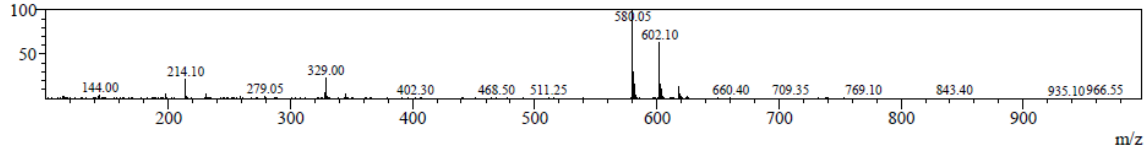

Figure S18 (c). LC-MS analysis of **20b**.

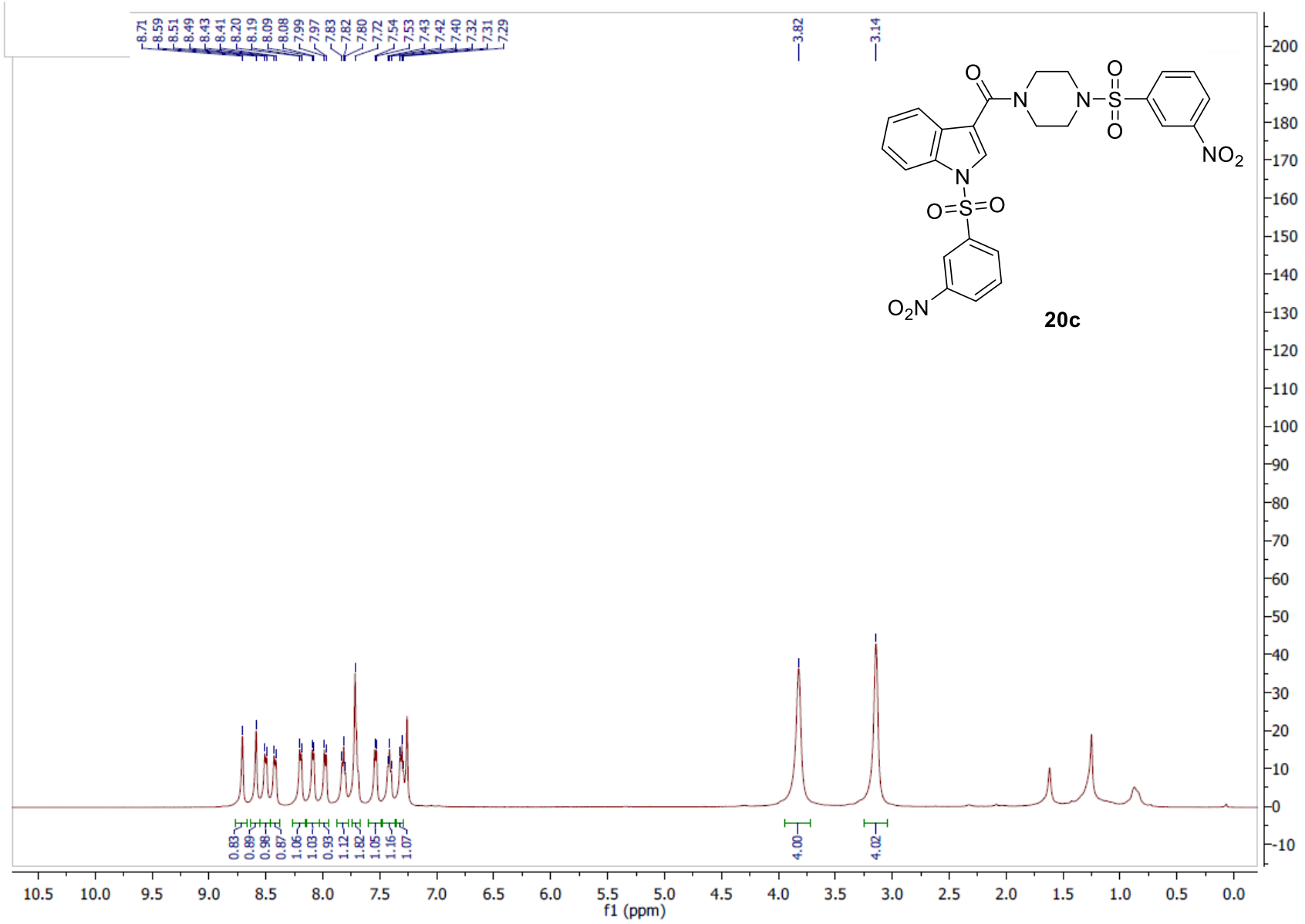

Figure S19 (a). ^{1}H NMR (500 MHz, $CDCl_3$) spectrum of **20c**.

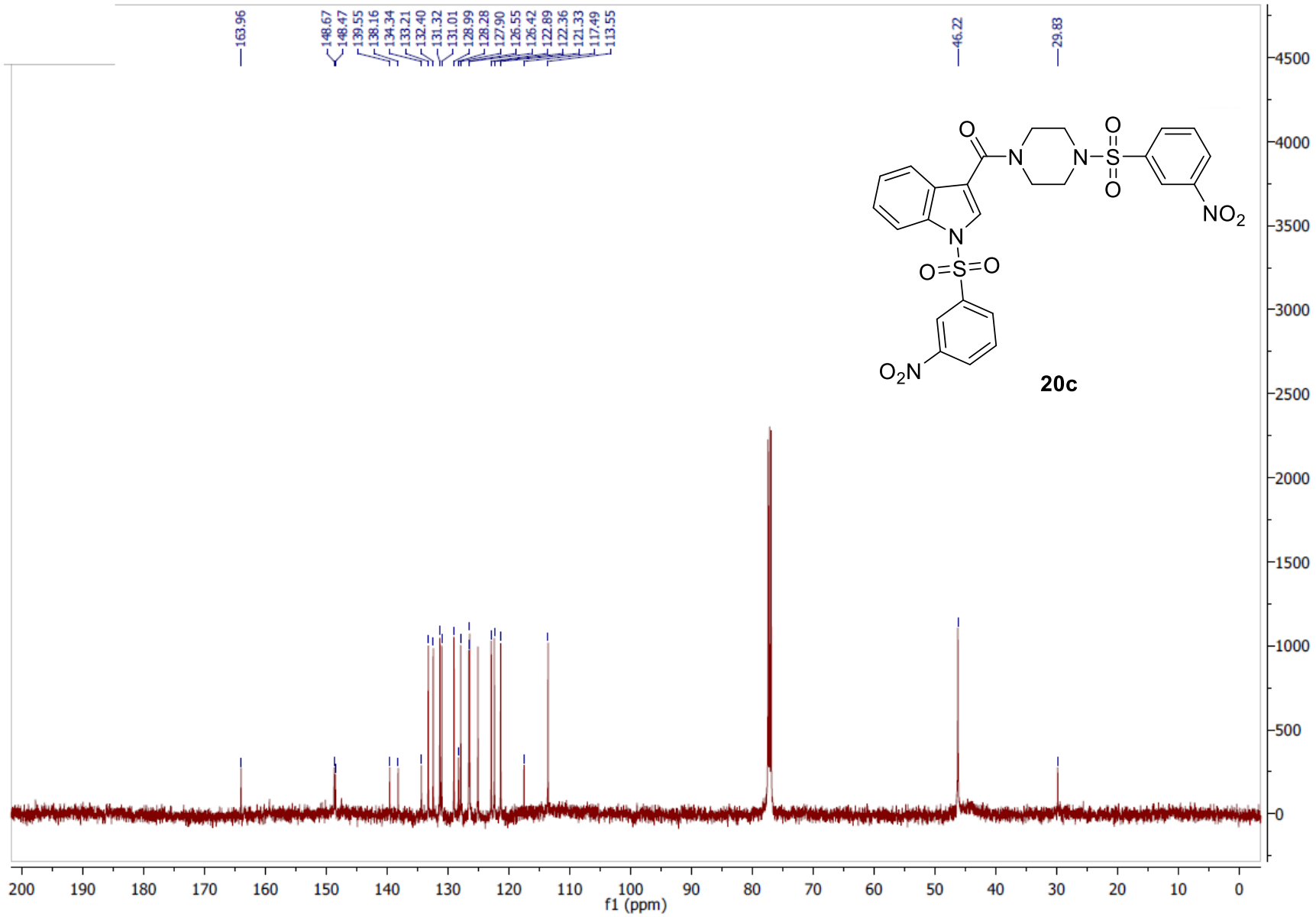

Figure S19 (b). ^{13}C NMR (125.7 MHz, $CDCl_3$) spectrum of **20c**.

==== Shimadzu LCMSsolution Analysis Report ====

Purospher-RP8

Sample Name : 91_94
Analysis Request :91_94_4
Data File Name : 91_94_4.lcd
Method File Name : ESI_grad_MeOH-aqCH3COONH4 10mM pH=3.9 formic.lcm
Data Acquired : 23/9/2014 1:26:34 μμ
Data Processed : 23/9/2014 2:11:41 μμ

Method

Column: Purospher C8, 25x4.6, 5um
Mobile Phase A: aq. CH3COONH4 10mM, pH=3.9 with formic acid
Mobile Phase B: MeOH
% Pump B Concetrate: 80.0
Flow (ml/min): 0.5000

Oven Temp.: 30
Detector A:SPD-20A
UV_1.Wavelength: 225
UV_2.Wavelength: 254
LC Program

Time	Unit	Command	Value
0.01	Pumps	B.Conc	80
20.00	Pumps	B.Conc	100
35.00	Pumps	B.Conc	100
35.01	Pumps	B.Conc	80
45.00	Pumps	B.Conc	80
45.01	Controller	Stop	

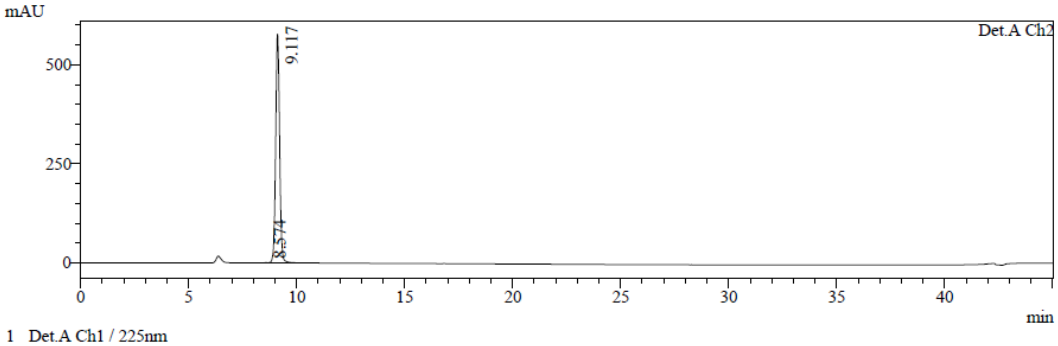

1 Det.A Ch1 / 225nm
2 Det.A Ch2 / 254nm

PeakTable

Detector A Ch1 225nm

Peak#	Ret. Time	Area	Height	Area %	Height %
1	9.115	9625855	756943	99.808	99.786
2	16.812	18510	1621	0.192	0.214
Total		9644365	758564	100.000	100.000

PeakTable

Detector A Ch2 254nm

Peak#	Ret. Time	Area	Height	Area %	Height %
1	8.574	6334	486	0.086	0.084
2	9.117	7385765	577311	99.914	99.916
Total		7392099	577797	100.000	100.000

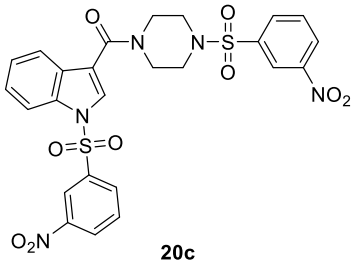

20c

MS Spectrum Graph

#:1 Ret.Time:Averaged 8.928-9.460(Scan#:975-1033)
BG Mode:Averaged 19.470-44.355(2125-4839)
Mass Peaks:350 Base Peak:157.05(1146817) Polarity:Pos Segment1 - Event1

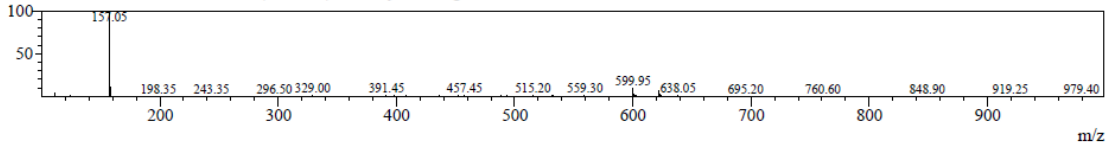

Figure S19 (c). LC-MS analysis of **20c**.